The Pennsylvania State University

The Graduate School

Department of Mechanical and Nuclear Engineering

MOLECULAR DYNAMIC SIMULATION OF ALUMINUM/WATER REACTION USING REACTIVE FORCE FIELD

A Thesis in

Mechanical Engineering

by

Rong Li

Submitted in Partial Fulfillment
of the Requirements
for the Degree of

Master of Science

May 2010

The thesis of Rong Li was reviewed and approved* by the following:

Matthew M. Mench
Associate Professor of Mechanical Engineering
Thesis Advisor

Adri van Duin
Associate Professor of Mechanical Engineering
Thesis Co-Advisor

H. Joseph Sommer III
Professor-In-Charge of MNE Graduate Programs
Professor of Mechanical Engineering
Thesis Reviewer

Karen A. Thole
Department Head of Mechanical and Nuclear Engineering
Professor of Mechanical Engineering

*Signatures are on file in the Graduate School

ABSTRACT

Over the past few years, it is becoming more likely that the emphasis on cleaner fuel will lead to use of hydrogen in a significant way. The worldwide increasing demand of hydrogen, such as in hydrogen fuel cells, has made it crucial to find hydrogen generation methods from inexpensive simple processes. One of the most promising approaches is hydrogen generation from the aluminum-water reaction. The hydrogen produced via such aluminum-water reactions can be employed to power fuel cell devices for portable applications such as emergency generators and laptop computers. Also, aluminum-water reactors can be used for emergency hydrogen storage on fuel cell-powered vehicles.

In this work, molecular dynamic simulations were conducted to study the aluminum-water reaction using the reactive force field (ReaxFF), which is optimized especially for Al and aluminum oxide. The initial reaction between water molecules and an Al cluster was considered to be the chemisorption of water molecules, and then the dissociation of adsorbed water molecules. Both water self-assisting effect and self poisoning effect on H_2O reaction are observed. The dissociation of adsorbed water molecule is assisted by other water molecules due to the interactions between them, which is referred to as water self-assisting effect on H_2O reaction. On the other hand, adsorbed water molecule can also prevent further reaction with the Al cluster, which is the water self poisoning effect. When too many water molecules are present in the system, considerable surface reaction sites are lost because of the chemisorption of water molecules. As a result, these adsorbed water molecules can't further dissociate, since the hydrogen atoms needs a free site to move into. The adsorbed water molecules tend to connect and form layers of water molecules starting from the adsorbed ones and stretching to the ones in the gas phase around the cluster. These layers of water molecules will also block the pathways for the reactants to arrive at the Al cluster surface.

Water dissociation (conversion) rate depends on the number of water molecules present in the system. The dissociation rate firstly increases with the number of water molecules because of the water self-assisting effect and then decreases with the number of water molecules due to water self poisoning effect. A maximum water dissociation rate of 100% is obtained for a 100 molecule Al cluster when 30 water molecules were originally added.

Among the intermediate species produced during the reaction, the hydronium ion is believed to be crucial to assist water molecule dissociation and facilitate hydrogen generation.

Acting as an inert specie, noble gas neon (Ne) was added to the aluminum-water mixture. Direct collisions between Ne atoms and water molecules are not observed, but Ne atoms can temporarily adsorb on the aluminum cluster. Due to water self-assistance and self poisoning effect, an optimum Ne concentration (corresponding to an optimum water concentration) is found with respect to higher water dissociation rate and hydrogen generation rate.

Different aluminum cluster sizes were also studied in this work. When the same average surface coverage of aluminum cluster by water molecules is maintained, higher water molecule dissociation rate and better hydrogen generation performance are obtained from larger aluminum cluster, due to the additional surface reaction sites provided by the larger aluminum cluster. However, for aluminum clusters with different sizes, the same optimum water concentration with respect to better water dissociation and hydrogen generation performance was found.

The influences of aluminum oxide layer on aluminum-water reaction are also investigated in this work. The presence of aluminum oxide layer causes the loss of available surface reaction sites, which is demonstrated by the reduction of chemisorption and dissociation of water molecules during the reaction. As the aluminum oxide layer becomes thicker, the spontaneous reaction of aluminum with water is severely prohibited or even stopped. To activate aluminum-water reaction, continuous removal of aluminum oxide either by mechanical or chemical methods is required. For future studies, modifying aluminum cluster structure or cluster surface configuration, or adding other materials to the aluminum cluster, may have the potential of promoting aluminum-water reaction.

TABLE OF CONTENTS

LIST OF FIGURES

LIST OF TABLES

ACKNOWLEDGEMENTS

I would like to thank Dr. Mench for welcoming me to his group during my difficult times. Without that, I would not have come so far today. Also, I would like to thank him for his continuous guidance and support on both my work and personal development.

I would like to thank Dr. van Duin for serving as my thesis co-advisor, for giving me the guidance and support for this work. I learned a lot from him.

Additionally, I would like to thank Dr. Russo for leading me through the MD simulations. The tutorials he wrote and the patient guidance he gave helped me during this work.

Finally, I would like to thank my family for their love and support throughout the years.

Chapter 1

Introduction

Considered as the world's clean energy choice, hydrogen holds the promise as a fuel with many potential social, economic and environmental benefits. Hydrogen fuel can be produced from clean and renewable energy sources; thus it has the long term potential to reduce the world's dependence on fossil fuel and energy-linked environmental impacts, like greenhouse emission, acid rain or ozone depletion. Hydrogen can also act as an energy storage medium, which is crucial to capture and store intermittent power from wind and solar energy.

Hydrogen has a wide variety of applications. It can be used either as the fuel for direct combustion, automobiles, power plants, thermal energy generation, or fuel for a fuel cell [1]. With a wide variety of applications, the world wide demand for hydrogen is increasing. Developing hydrogen production technologies that can be implemented in a sustainable, clean and economic manner will be crucial in order to meet the growing needs for hydrogen.

1.1 Hydrogen Generation Mechanisms

Although hydrogen is the most abundant element in the universe, elementary hydrogen gas is hardly found on earth [2]. It is therefore necessary to produce hydrogen from other hydrogen-containing compounds such as fossil fuels, biomass, or water. There are a number of categories into which hydrogen production methods can be divided. They can be divided into thermal, electrolytic and photochemical processes. They can also be divided by different main supplies: fossil fuel and chemical; renewable energies and electrolytic processes; biological systems; and nuclear fission or fusion incorporating electrolytic production or chemical methods [3].

1.1.1 Hydrogen Generation form Fossil Fuels

Hydrogen has been produced from fossil fuels historically, and approximately 95% of the hydrogen produced today comes from carbonaceous raw material, primarily fossil in origin. The world production of hydrogen is approximately 50 million tones annually and most of this amount results from reforming of natural gas [3]. Mostly, the hydrogen is produced by steam reforming. The basics of this process involve the mixture of natural gas with water steam where molecular H_2 is freed from both components [4]. In the USA, approximately 95% of all hydrogen is produced by steam reforming of natural gas [3]. Another method is partial oxidation, which is mostly used for heavy feeds like coals and heavy hydrocarbons. When mixing the methods of reforming and partial oxidation, a third method is called the auto-thermal reforming (ATR) process. In general, the partial oxidation and ATR are least demanding in terms of hardware space of the reforming technologies.

The afore-mentioned methods can take advantage of the currently least expensive and most established techniques for the large-scale hydrogen production. They can be used in the foreseeable future to meet hydrogen fuel demand and to enable the testing of technologies related to hydrogen production, storage, distribution, safety and application.

However, each of these three hydrogen production methods emits carbon dioxide as a by-product, which is believed by many to be the principal cause of global climate change. This is the main concern with manufacture of hydrogen from fossil fuels using reformation and gasification processes. In the long term, there is a growing concern about the shortage of fossil fuel for the generations to come. Known reserves of oil and natural gas may last 40 years at the current rate of consumption [5, 6]. However, the growth in world population has resulted in an increase of 35% in world oil demand over the past 30 years [5, 6]. Accounting for the population growth and its impact on oil demand, it is clear that the world oil production cannot be sustained indefinitely at its current rate [7]. To achieve the benefits of a truly sustainable hydrogen energy economy, it is necessary and crucial to move to a situation where hydrogen is produced from non-fossil resources.

1.1.2 Hydrogen Generation from Biomass

Biomass is potentially a reliable energy resource for hydrogen production. It is renewable and relatively easy to use. Major resources in biomass include agricultural crops and their waste byproducts, lignocellulosic products such as wood and wood waste, waste from food processing and aquatic plants and algae, and effluents produced in the human habitat [1]. The portion of the hydrogen in the biomass depends strongly on the different feedstock [3].

There are two major methods available for hydrogen production from biomass: thermochemical and biological processes [3]. Combustion, pyrolysis, liquefaction and gasification are the four thermochemical processes. Direct biophotolysis, indirect biophotolysis, biological water–gas shift reaction, photo-fermentation and dark-fermentation are the five biological processes [8]. The thermochemical pyrolysis and gasification hydrogen production methods are economically viable and believed to be competitive with the conventional natural gas reforming method. Biological dark fermentation is also a promising hydrogen production method for commercial use in the future [8]. Although hydrogen production from biomass is clearly attractive, the main hurdle in adopting these processes is the relatively low energy conversion efficiencies and unstable hydrogen production.

1.1.3 Hydrogen Generation from Water Electrolysis

Water electrolysis is the process of breaking the bonds of the water molecule and separating it into hydrogen and oxygen. Although it is technologically very simple and delivers very clean gases, because of high electricity consumption, hydrogen generation from water electrolysis is not cost-effective. The energy required to break the bonds of water and separate it into its elementary constitutes amounts to approximately 33kWh per kilogram of water [3]. The cost of hydrogen by electrolysis of water is currently several times higher than that produced from fossil fuels [9, 10].

Considerable research is ongoing to make electrolytical production to become an attractive one [11, 12]. Possible approaches for reduction of energy required in the water electrolysis process include zero-gap cell geometry, development of new diaphragm materials and especially development of new electrocatalytic materials for the electrodes. Another approach is

making the electricity as inexpensive as possible [11, 12]. In some countries, where there is excess production capacity, the electricity price is lower.

The use of wind and solar energy to produce hydrogen is seen by many as applicable in the future. However, the stability of wind and solar energy is limited. Further, the costs of wind-based hydrogen are rather difficult to assess accurately; and solar to hydrogen conversion efficiencies can vary in a large range [3].

1.2 Hydrogen Generation from Metal Water Reaction

Over the years, the concept of hydrogen generation from chemical reactions of reactive metals, including Zn, Mg, and Al, has been receiving increasing interests [13-20]. In these reactions, hydrogen will be extracted from the hydrogen sources such as water or hydrocarbons with the help of metals of high activity.

1.2.1 Mechanism of Hydrogen Generation from Aluminum-Water Reaction

Among the different metals, aluminum has been identified to be the most promising candidate for the purpose of hydrogen generation [21]. Being the most abundant crustal metal on earth, aluminum and its alloys possess a number of valuable mechanical, electrical and thermal properties [22]. They are widely used in various areas, transportation, building, electrical engineering, and so on. With its low density of 2700 kg/m^3, aluminum is the lightest among all the commonly used metals [22]. Such a property helps achieve a significant reduction in the total weight of a system. Another important fact is that the cost of aluminum based hydrogen production is reasonable for certain applications (See Appendix B). There is also the suggestion that aluminum-water reactions might be used for hydrogen storage on fuel cell-powered vehicles, although the relative cost compared to gasoline is probably high.

The following are some possible reactions of aluminum with water [23]:

$$2Al + 6H_2O \rightarrow 2Al(OH)_3 + 3H_2 \quad (1.1)$$

$$2Al + 4H_2O \rightarrow 2AlO(OH) + 3H_2 \quad (1.2)$$

$$2Al + 3H_2O \rightarrow Al_2O_3 + 3H_2 \quad (1.3)$$

1.2.2 Chemical and Mechanical Activation Methods for Aluminum-Water Reaction

From a thermodynamics point of view, aluminum should spontaneously react with water. However, due to strong affinity for oxygen [13], an adhering layer of aluminum oxide is usually formed on the surface of aluminum, which prevents its reaction with water.

Considerable research is focusing on the approaches of promoting aluminum-water reaction [23-51]. Generally, both chemical activation and mechanical activation of aluminum have been based on the idea of continual removal and disruption of the aluminum oxide layer. Currently, there have been modified Al products especially developed for promoting aluminum-water reactions available in the market, although the fundamental understanding of the promoting reaction mechanisms is not yet completely accomplished.

1.2.2.1 Hydroxide Promoters

In alkaline solutions, aluminum oxide or aluminum as well are readily dissolved, which will result in hydrogen production. That is why considerable research has been focusing on using hydroxide, primarily sodium hydroxide to promote aluminum-water reaction [24-28]. Also several hydrogen generation devices have been developed based on the reaction mechanisms [29-37]. The series of reactions found to occur between aluminum, sodium hydroxide and water are shown below:

$$2Al + 2NaOH + 2H_2O \rightarrow 2Na_2Al_2O_4 + 3H_2 \quad (1.4)$$

$$2Al + 6NaOH + xH_2O \rightarrow Na_6Al_2O_6 + xH_2O + 3H_2 \quad (1.5)$$

$$2Al + 2NaOH + 6H_2O \rightarrow 2NaAl(OH)_4 + 3H_2 \quad (1.6)$$

$$2NaAl(OH)_4 \rightarrow 2NaOH + 2Al(OH)_3 \quad (1.7)$$

$$2Al + 6H_2O \rightarrow 2Al(OH)_3 + 3H_2 \quad (1.8)$$

The formation of sodium aluminate was observed for hydrogen generation reactions (1.4) and (1.5). Reactions (1.6) and (1.7) are suggested to be involved in hydrogen generation processes [38-40]. If the reaction is properly controlled, the regeneration of $NaOH$ in reaction (1.7) will essentially cover the depletion of it in reaction (1.6). Therefore, for hydrogen generation, only water and aluminum are consumed, shown in reaction (1.8).

Numerous studies have focused on the various parameters which affect hydrogen production via this method, among which temperature and alkaline concentration are considered as the crucial ones [41]. Several comprehensive parametric studies can be found in [42, 43].

1.2.2.2 Oxide Promoters

In comparison with those reactions assisted by alkalis, the use of oxide promoters is much safer. The aluminum oxide promoters may be in the form of bayerite ($Al(OH)_3$), boehmite ($AlO(OH)$), gamma alumina ($\gamma - Al_2O_3$) or alpha alumina ($\alpha - Al_2O_3$) [23]. However, recent research has suggested that the enhancing effect of aluminum oxide on the reactivity of aluminum with water may also be mechanochemical in nature [44].

It has also been shown that heavily ball-milled Al-Al_2O_3 powder mixtures are reactive with water in the PH range of 4-9 and at temperatures of 10-90^{0}C [45-47]. The ball milling is a process in which materials are fractured into small powders under the action of high energy ball-powder collisions. It will increase the exposed specific surface area and disrupt the oxide layers present on the aluminum powder.

1.2.2.3 Salt Promoters

Since water soluble inorganic salts can produce localized pitting and rupture of the alumina layer on the aluminum particles [48, 49], they have been employed to promote hydrogen production from aluminum-water reactions. Among the salts investigated, NaCl and KCl are suggested to be the most effective [50, 51]. Powders of these salts were ball-milled together with aluminum powder in a proper weight ratio. The ball-milled process will also destroy the alumina layers on the aluminum particles, thus further activating the aluminum reaction with water.

1.3 Objectives

As the worldwide need for electricity increases, a hydrogen-based economy is the promising long term, environmentally benign alternative for sustainable growth.

Among the traditional and newly developed hydrogen generation methods reviewed in this chapter, the aluminum-water reaction has the potential of producing hydrogen in a relatively cost effective, convenient, and environmental friendly manner. The hydrogen produced via aluminum-water reaction might be employed for hydrogen storage on fuel cell-powered vehicles, and also can be applied to power fuel cell devices for portable applications such as emergency generators and laptop computers.

However, to the best of knowledge, the fundamental understanding about aluminum-water reaction is not yet fully accomplished. Therefore, based on research of the following aspects:

a) the influencing parameters of the aluminum-water reaction analyses,
b) water concentration analyses
c) noble gas concentration analyses
d) aluminum particle size analyses
e) aluminum oxide layer effect analyses

the main objective of this work is to study the mechanisms of aluminum-water reaction at a molecular level, which is crucial for future applications of aluminum-water reaction.

Chapter 2

Method of Approach

The Molecular Dynamic (MD) simulation calculates the time dependent behavior of a molecular system and generates information at the microscopic level. It gives understanding of dynamical properties of the system including transport coefficients, time-dependent responses to perturbations, rheological properties and spectra.

2.1 Introduction to Molecular Dynamic Simulations

Molecular dynamics simulation consists of the numerical, step by step, solution of the classical equations of motion:

$$F_i = m_i a_i \tag{2.1}$$

$$F_i = -\frac{\partial U}{\partial r_i} \tag{2.2}$$

$$a_i = \frac{\partial^2 r_i}{\partial t^2} \tag{2.3}$$

$$-\frac{\partial U}{\partial r_i} = m_i \frac{\partial^2 r_i}{\partial t^2} \tag{2.4}$$

where F_i is the force exerted on the particle i, m_i is its mass, r_i and a_i are its location and acceleration. From the knowledge of the force on each atom, it is possible to determine the acceleration of each atom in the system. Integration of the equations of motion then yields a trajectory that describes the positions, velocities and accelerations of the particles as they vary with time. From this trajectory, the average values of properties can be determined. The method is deterministic; once the positions and velocities of each atom are known, the state of the system can be predicted at any time in the future or the past. The force F_i acting on the atoms can be

calculated form the potential energy $U(r^N)$ function, where $r^N = (r_1, r_2, r_3 \cdots r_N)$ represents the complete set of $3N$ atomic coordinates [52].

2.2 Introduction to Reactive Force Field (ReaxFF)

As discussed earlier, a MD simulation requires the definition of a potential function, or a description of the terms by which the particles in the simulations will interact. In the chemistry and biology applications, this is usually referred to as a force field. In the context of molecular mechanics, a force field refers to the functional form and parameter sets used to describe the potential energy of a system of particles (typically but not necessarily atoms). One of the most important features of the ReaxFF, reactive force field, is a capability to describe chemical reactions in composite systems with a wide variety of constituents, including metals and polymers, with the same set of force field parameters.

The main difference between traditional unreactive force field and ReaxFF is that the connectivity is determined by bond orders calculated from interatomic distances that are updated every MD step [53]. ReaxFF is a general bond-order-dependent force field that provides accurate descriptions of bond breaking and bond formation. The elements of ReaxFF are [53]:

a) charge distributions change instantaneously as atomic coordinates change
b) all valence interactions use bond orders derived uniquely from the bond distances which in turn describe uniquely the energies and forces
c) three body (angle) and four body (torsion and inversion) terms are allowed but not required
d) a general “van der Waals” term describes short range Pauli repulsion and long range dispersion interactions, which with Coulomb terms are included between all pairs of atoms (no bond or angle exclusions)
e) no environmental distinctions are made of atoms involving the same element

The ReaxFF framework employed in this work was initially developed for hydrocarbons [54]. Since then, it has been successfully applied to accurately predict the dynamical and reactive processes in hydrocarbons [54], nitramines [55], silicon/silicon oxides [56], aluminum/aluminum oxides [55], and a wide range of other systems. The ReaxFF framework employs instantaneous bond orders, including contributions from sigma, pi and double-pi bonds, which are calculated from the interatomic distance. These instantaneous bond orders are subsequently corrected with

over-coordination and under-coordination terms to force systems towards the proper valency. These bond orders are updated every MD-iteration, thus allowing ReaxFF to recognize new bonds and to break existing bonds [55].

In this study, the force field parameters used were optimized for aluminum and aluminum oxide within the ReaxFF scheme. One of the most important features of this set of ReaxFF parameters is that they are fully transferable. They can be applied not only for a metal/oxide interface, like in study [57] for aluminum and aluminum oxide, but also for studying the oxidation of aluminum and the hydration of $\alpha - Al_2O_3$, and how aluminum or aluminum oxide interacts/reacts with Si, SiO_2, hydrogen, hydrocarbons, and other organic molecules for which the parameterization is available. Therefore, this force field is well transferable to situations where reactions of H and H_2O with Al and Al_2O_3 are of interest, which is exactly the case in this study.

2.3 Aluminum Cluster Preparation

The original aluminum clusters are built up from geometries constructed from an aluminum face centered cubic (fcc) crystal. According to the density of the aluminum, the radius of aluminum sphere which contains the number the aluminum atoms of interest can be calculated. The spherical sample obtained at this stage is still in the perfect layers of the crystal lattice from which it was created, shown is Figure **2-1**. This aluminum cluster structure is not practical. For the atoms on the edge of the sphere, they have been taken out of the bulk and only have a fraction of neighbor atoms, which they used to have when they were in the bulk crystalline phase. Therefore, before allowing any reactions to take place, the aluminum clusters must be prepared to transform to their realistic configuration.

The annealing process is carried out by using an optional ReaxFF file called ‘tregime.in’, which defines the segment of the aluminum cluster for the annealing process, time step, heating rate, and the temperature damping constant. Shown in Figure **2-2**, the aluminum cluster is first heated up to its melting temperature by a heating rate 0.01K per time step, then the temperature is kept around the melting temperature at 800K for a certain period of time. This stage is designed to allow the aluminum cluster to catch up with the desired temperature (there is some lag due to the temperature damping constant), and provide enough time for the surface to rearrange itself

and for the edge atoms to migrate to a more stable and realistic configuration. It is also crucial to have a smooth transition between the heating and cooling processes. After 70000 steps maintaining at the melting temperature, a new zone is initiated in which the aluminum cluster is cooled down by a cooling rate of -0.01K per time step. In Figure **2-3** and Figure **2-4**, it shows that the aluminum cluster is at a lower energy state at the end of annealing process, which means the annealed aluminum cluster is at a more stable state and in a more realistic configuration.

Applying the aluminum cluster structure obtained from the first annealing as a starting point; a second annealing process is carried out. The goal is to make sure the configuration obtained from the first annealing is indeed stable. Figure **2-5** shows the temperature of aluminum cluster during the second annealing process. In Figure **2-6** and Figure **2-7**, the total energy of the aluminum cluster at the end of the second annealing is the same as that at the beginning of the second annealing. It indicates the aluminum cluster is already at the lowest energy state after first annealing. Therefore, the double annealing process produces a stable configuration of the aluminum cluster, which is shown in Figure **2-8**, for the subsequent MD simulations.

2.4 Formulation of Simulation Cases

The aluminum-water reaction is important to many combustion and explosive systems, and considerable research is ongoing in these fields. However, there is still considerable uncertainty remaining in the understanding of the reaction mechanism of aluminum with water at molecular level. With the help of ReaxFF, which was developed especially to describe chemical reactions in composite systems with a wide variety of constituents, the main objectives of this paper are to study the roles of water concentration, noble gas concentration, aluminum particle size, and aluminum oxide layer playing in the reaction of aluminum with water.

2.4.1 Water Concentration

Understanding how water molecules react with aluminum particle and the reaction behavior of the water molecules around aluminum particle will certainly facilitate future efforts to study the reaction mechanisms and help the design of future technological devices for hydrogen production through aluminum-water reaction.

In this work, the number of water molecules added to the same aluminum cluster is controlled to form a set of simulations. The phenomenon to be studied are the initial reaction between a water molecule and aluminum cluster, the chemisorption of water molecules, the decomposition of adsorbed water molecules on the aluminum cluster surface, the generation of intermediate species, the possible reactions between water molecules and the intermediate species, and the dissociation rate of water molecules during the reaction. The set of simulations carried out is listed in Table **2-1**.

2.4.2 Noble Gas Concentration

Noble gas Ne is added into the reaction system to control the water molecule concentration and to control water reaction rate. The following studies are carried out including how noble gas interacts with aluminum cluster, how noble gas atoms affect aluminum-water reaction, what are the interactions between water molecules and noble gas molecules, and also regarding to aluminum-water reaction promotion, what is the optimum ratio of water molecule to noble gas molecule. For this set of simulations, Table **2-2** and Table **2-3** summarize all the cases studied. A general guide line is followed for setting up the simulation cases. For the same aluminum cluster, the simulation of the influence of water concentration, which is defined as the ratio of the number of water molecules to the total number of water molecules and Neon atoms, is carried out. Three different water concentrations were applied, 0.25, 0.5, and 0.75.

2.4.3 Aluminum Particle Size

It is known that the reactions of metal clusters with small molecules often depend on cluster size [58]. The use of nano-sized particles in the aluminum-water reaction can offer significant advantages over large size particles. Much of the highly desirable traits of nano-sized metal powders can be attributed to their high specific surface area and overall small dimensions.

In this study, five aluminum clusters for conducting MD simulations were prepared. They are listed in Table **2-4**. The original aluminum clusters were built up from geometries constructed from an aluminum face centered cubic crystal, and then were treated with two annealing processes, in which enough time is provided for the surface to rearrange itself and for the edge

atoms to migrate to a more stable and realistic configuration. After annealing, the aluminum clusters are ready to be applied in MD simulations of reactions with water, noble gas, as well as oxygen.

Understanding how a specific size or shape will affect the reactivity of aluminum cluster towards water may facilitate future efforts to design stable or reactive aluminum particles for specific technological applications.

2.4.4 Aluminum Oxide Layer

Because of their strong affinity for oxygen, aluminum and its alloys are usually well protected by a thin coherent, adhering layer of aluminum oxide Al_2O_3 formed on their surfaces; and this alumina layer prevents the further reaction of aluminum with water. A considerable amount of research is focusing on approaches promoting aluminum-water reaction by continual removal and disruption of the aluminum oxide layer [23-37, 44-47]. The main prospective of this work is to study how the aluminum oxide layer will affect aluminum-water reaction at a molecular level, how it will influence the hydrogen generation, and whether the thickness of the oxide layer would have a strong influence on the reaction rate.

During the first stage of the simulation, oxygen molecules are added into the system and the simulation with only oxygen and aluminum cluster proceeds first. After a certain period of time, there will be aluminum oxide layer formed on the aluminum surface. Then in the second stage of the simulation, water molecules are introduced into the system, and then the simulation with water molecules and aluminum cluster with aluminum oxide layer is carried out later on in the reaction system. The thickness of the aluminum oxide layer is controlled by the oxygen molecules added into the system at the first place and also by the reaction time of the first stage. The simulation cases are listed in Table **2-5**.

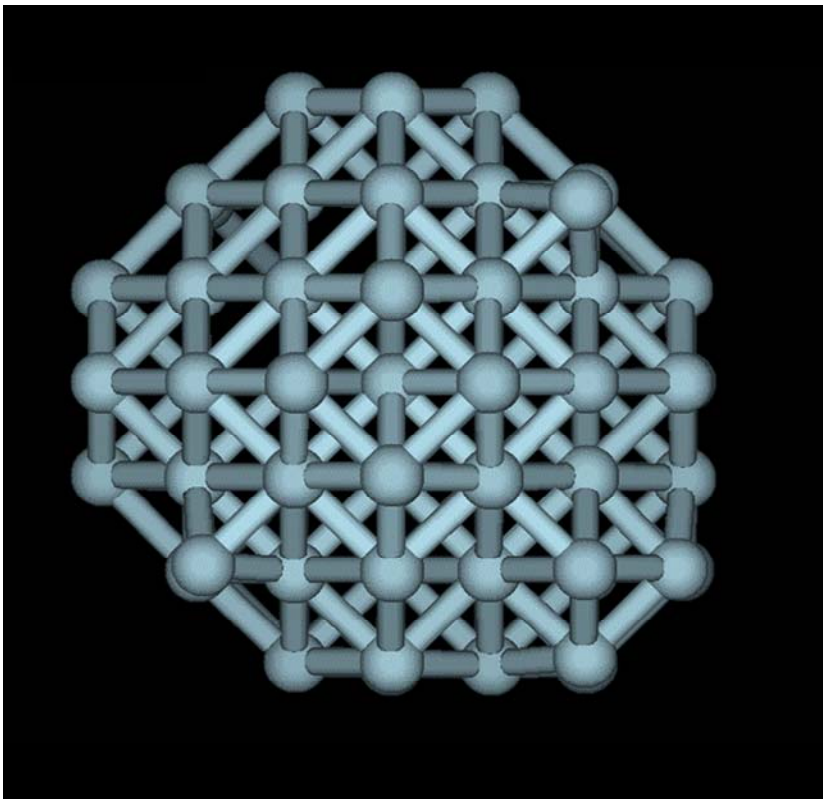

Figure 2-1: Aluminum cluster obtained from an aluminum face centered cubic (fcc) crystal

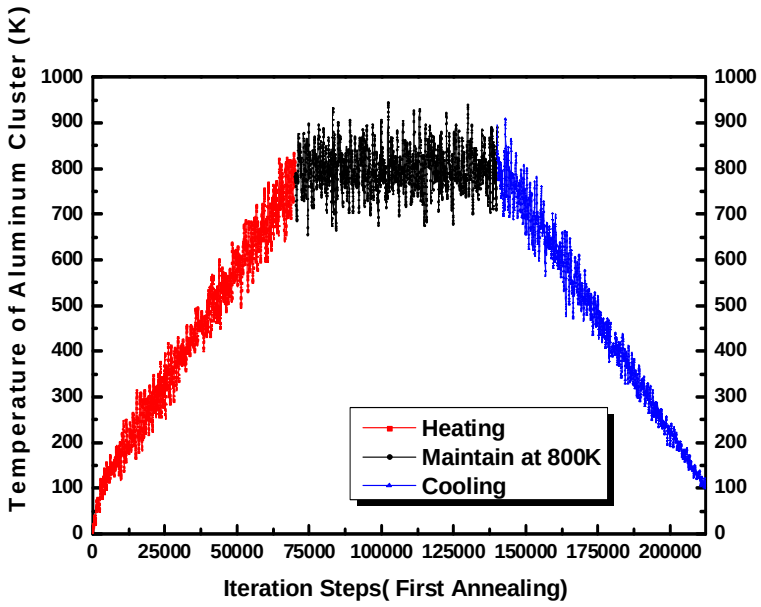

Figure 2-2: Temperature profile of aluminum cluster during first annealing process

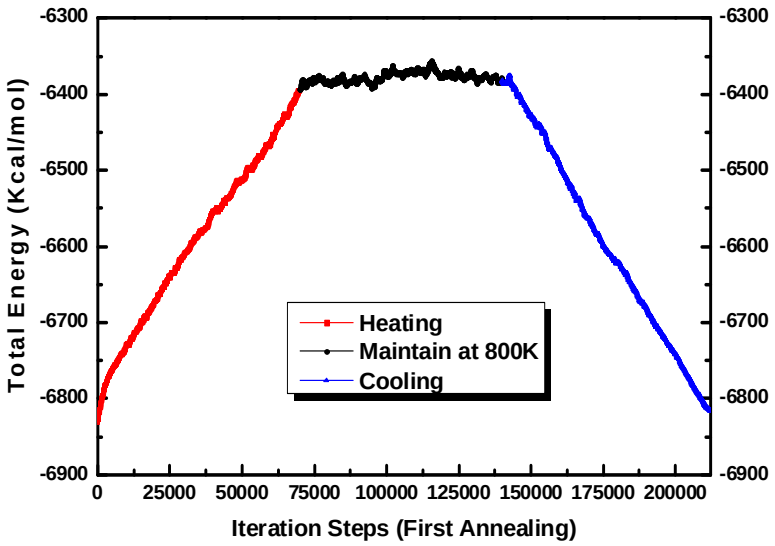

Figure 2-3: Profile of aluminum cluster total energy during first annealing process

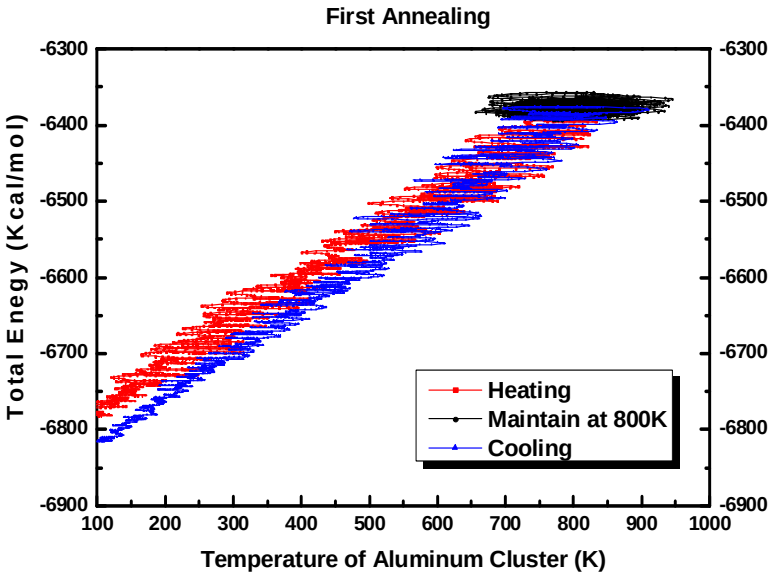

Figure 2-4: Total energy versus temperature of aluminum cluster during first annealing process

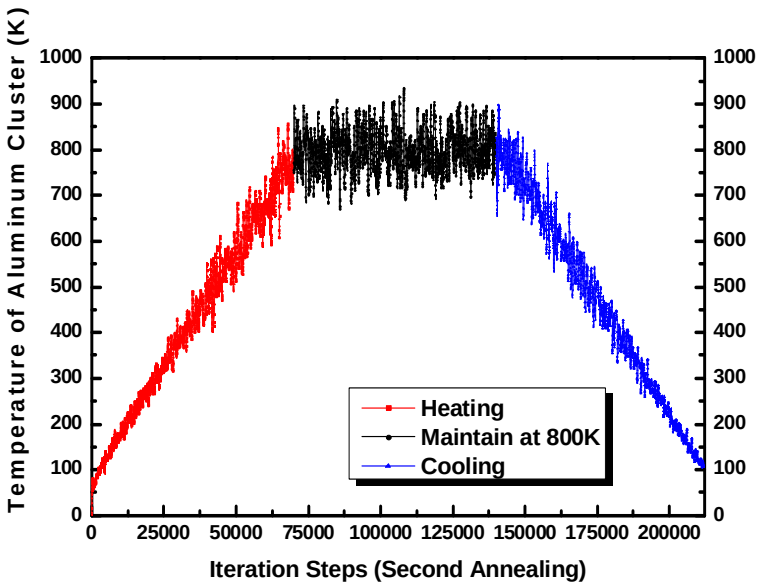

Figure 2-5: Temperature profile of aluminum cluster during second annealing process

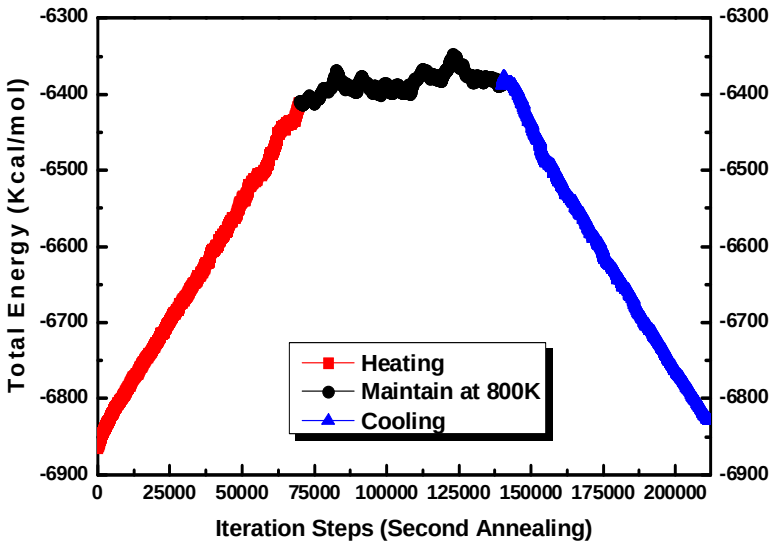

Figure 2-6: Profile of aluminum cluster total energy during second annealing process

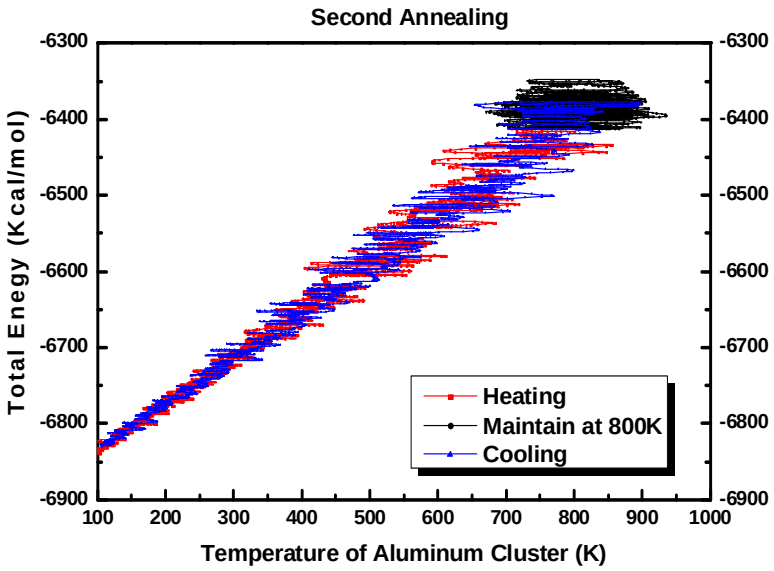

Figure 2-7: Total energy versus temperature of aluminum cluster during second annealing process

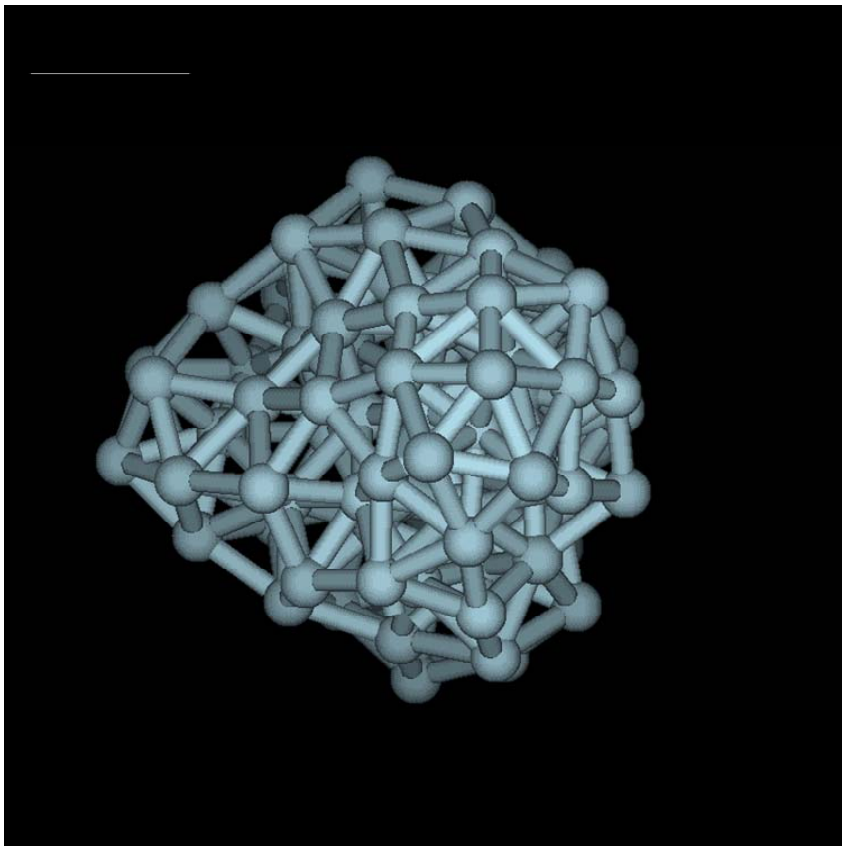

Figure 2-8: Stable aluminum cluster structure after annealing

Table **2-1**: Simulation Cases for Water Conversion Rate Analysis

Aluminum Cluster	Number of Water Molecules Added
Al100	10
Al100	20
Al100	30
Al100	40
Al100	50
Al100	62
Al100	75
Al100	87
Al100	100

Table **2-2**: Simulation Cases for Noble Gas Concentration Analysis (Al100)

Aluminum Cluster	Number of Water Molecules Added	Number of Ne Atoms Added
Al100	100	0
Al100	75	25
Al100	50	0
Al100	50	12
Al100	50	25
Al100	50	50
Al100	25	75

Table **2-3**: Simulation Cases for Noble Gas Concentration Analysis (Al200)

Aluminum Cluster	Number of Water Molecules Added	Number of Ne Atoms Added
Al200	160	0
Al200	120	40
Al200	80	80
Al200	40	160

Table **2-4**: Simulation Cases for Noble Gas Concentration Analysis

Aluminum Cluster	Number of Water Molecules Added	Number of Ne Atoms Added
Al100	100	0
Al100	75	25
Al100	50	0
Al100	50	12
Al100	50	25
Al100	50	50
Al100	25	75
Al200	160	0
Al200	120	40
Al200	80	80
Al200	40	160
Al300	208	0
Al300	156	52
Al300	104	104
Al300	52	156
Al400	252	0
Al400	189	63
Al400	126	126
Al400	63	189
Al500	300	0
Al500	225	75
Al500	150	150
Al500	75	225

Table **2-5**: Simulation Cases for Aluminum Oxide Layer Influence Analysis

Aluminum Cluster	Number of O_2 Molecules Added	Number of Water Molecules Added
Al100	25	50
Al100	50	50
Al100	79	50

Chapter 3

Results and Discussion

3.1 Reactive Behavior of Water Molecules with Aluminum Particles

The reaction of aluminum with water is a fundamentally complex system. In this work, by adjusting the number of water molecules added into the system as well as the water concentration, the reaction mechanism and kinetics of the water dissociation reaction are studied.

3.1.1 Reaction Assistance of Water Molecule

Figure **3-1** shows the variation of number of adsorbed water molecules onto the Al100 cluster as simulation continues. Initially, the adsorption of water molecules onto the Al cluster is observed and then a dissociative process of adsorbed water molecules is followed. This explains why the number of adsorbed water molecules on Al100 cluster first increases and then decreases as the simulation proceeds. Also, for the cases with higher number of water molecules, the water dissociation slows down, leading to a larger amount of chemisorbed water molecules at the end of the simulation.

Besides from chemisorption onto the Al cluster, water molecules tend to connect with each other through temporary hydrogen bonds to form large area of water molecule layer (or several layers), which is shown in Figure **3-2**. This layer can prevent water molecules from reacting with Al cluster since it blocks the pathways of water molecules to get to the Al surface.

3.1.2 Reaction Mechanism of Adsorbed Water Molecules

It is crucial to understand the reaction mechanism of adsorbed water molecules, since it mainly determines the generation of intermediate species in the system. In the simulations, it is observed that a water molecule is adsorbed to the Al cluster through O-Al bond, which is shown

in Figure **3-2** and Figure **3-3**. The adsorbed water molecules can desorb from the Al cluster and then re-adsorb to the cluster again. Here, (ads) is used to represent the atom or the molecule which is adsorbed to the Al cluster, and (g) is used to indicate the atom or molecule which is in the gas phase. Direct dissociation of adsorbed water into OH (ads) and H (ads) is not observed. Instead, the adsorbed water molecule dissociates into OH (ads), hydroxyl and releases one proton to the water-phase to make a solvated H_3O-cation. The dissociation process is shown in series of snapshots in Figure **3-3**, and the dissociation reaction can be expressed as:

$$H_2O(ads) \rightarrow OH(ads) + H(g) \quad (3.1)$$

$$H(g) + H_2O(g) \rightarrow H_3O(cation, g) \quad (3.2)$$

The dissociation process of adsorbed water molecules may be facilitated by the interactions between the adsorbed water molecules and the intermediate species in the gas phase, which will be further discussed below.

3.1.3 Formation of Al-H bond

From previous discussions, it is known that the adsorbed hydrogen atoms are not directly formed from the dissociation process of adsorbed water molecules. However, the formation of Al-H bond is found on the Al Cluster. Figure **3-4** illustrates the formation process of adsorbed hydrogen atoms on the Al cluster. The hydrogen atoms in the gas phase can easily adsorb to Al cluster, which is expressed in Reaction **3.2**.

$$H(g) \rightarrow H(ads) \quad (3.3)$$

The source for hydrogen atoms in the gas phase can either be the dissociation of adsorbed water molecules, or the dissociation of water molecules in the gas phase or dissociation of generated hydrogen in the gas phase.

Unlike the adsorbed hydroxyl on Al cluster, the adsorbed hydrogen atom is highly mobile on the cluster surface. It migrates on the cluster surface through forming and breaking Al-H bonds, which are formed between the adsorbed hydrogen atom and different Al atoms on the cluster surface. Figure **3-5** clearly shows how the adsorbed hydrogen atoms migrate on the Al cluster surface.

3.1.4 Formation of Hydronium Ion H_3O (cation, g) and the Related Surface Reactions

There are many intermediate species formed during aluminum-water reaction, one of which that is considered to be the most important is hydronium ion ($H_3O(cation, g)$). It assists the dissociation of water molecules and initiates the formation or consumption of other intermediate species in the reaction system.

3.1.4.1 Formation Mechanisms of $H_3O(cation, g)$

The hydronium ion is formed through the reaction between the adsorbed water molecule and the water molecule in the gas phase, shown in reaction (3.4). The adsorbed water molecule dissociates into one proton, which is captured by the water molecule in the gas phase to form a hydronium ion, and one hydroxyl which is still adsorbed to the Al cluster. This formation process is shown in Figure **3-6**.

$$H_2O(ads) + H_2O(g) \rightarrow OH(ads) + H_3O(cation, g) \quad (3.4)$$

3.1.4.2 Surface Reactions Involving $H_3O(cation, g)$ -Hydrogen Generation

The hydronium ion participates in multiple surface reactions, one of which is hydrogen generation reaction. Shown in reaction (3.5), when hydronium ion reacts with adsorbed water molecules, dissociation process takes place for both molecules. The adsorbed water molecule dissociates into hydroxyl, which is adsorbed to the cluster and hydrogen atom which will combine with the other hydrogen atom dissociating from the hydronium ion to form hydrogen gas. Losing one hydrogen atom, the hydronium ion recovers to a water molecule in the gas phase. Figure **3-7** contains the snapshots capturing the event.

$$H_3O(cation, g) + H_2O(ads) \rightarrow OH(ads) + H_2O(g) + H_2(g) \quad (3.5)$$

3.1.4.3 Surface Reaction Involving $H_3O(cation, g)$ - Al-H Bond Formation

Either one of the three identical hydrogen atoms in the hydronium ion can separate from the ion and react with other species in the system. If the breaking-away hydrogen atom is adsorbed to the Al cluster, an Al-H bond is formed. Figure **3-8** shows the formation process.

Generally speaking, the intermediate hydronium ion $H_3O(cation, g)$ has three identical hydrogen atoms, and is capable of reacting with both reactants and intermediate species. The hydronium ion reacts with water molecules both in the gas phase and adsorbed to the Al cluster, with hydrogen gas, with hydrogen atoms in the gas phase and with hydronium ion itself. It is a key intermediate in the aluminum-water reaction system.

3.1.5 Water Self-Poisoning Effect

As discussed earlier, the interactions between a water molecule and Al cluster are considered to be the adsorption of a water molecule onto the Al cluster and subsequently a dissociative process of the adsorbed water molecule. A decent amount of water molecules is needed for the generation of intermediate species and substantially the hydrogen production. By increasing the water molecules added into the system to a certain extent will promote the reaction. However, further increasing the number of water molecules added into the gas phase is proved to be inefficient regarding to reaction enhancement. The different influences associated with the number of water molecules participating in the reaction were attributed to water self poisoning when too much water is added into the reaction system.

For Al100 cluster, there are roughly about 50-60 sites available for surface reaction. When too many water molecules are present in the system, all these available reaction sites are fully occupied by adsorbed water molecules. As a result, these adsorbed water molecules can not dissociate any more, since the hydrogen atoms needs a free site to move into. Figure **3-9** and Figure **3-10** show the variations of the number of adsorbed hydroxyl and the number of broken OH bonds as reaction continues for different cases, in which different numbers of water molecules were added initially. In Figure **3-1**, the number of adsorbed water molecules increases with the initial water addition throughout the reaction. However, in Figure **3-9** and Figure **3-10**, it is shown that from the point at which the number of water molecules is 75 on, the number of adsorbed hydroxyl and the number of broken OH bonds both decrease. It means that the

dissociation of water molecules is hindered. As a result, the hydrogen generation is also impeded because of water self poisoning, which is shown in Figure **3-11**.

Besides from adsorbing to Al cluster, as shown in Figure **3-2**, water molecules tend to connect with each other and form layers and layers of water molecules starting from the adsorbed ones and stretching to the ones in the gas phase around the cluster. These layers of water molecules will also block the path ways for free water molecules in the gas phase to arrive at the Al cluster surface, and subsequently interrupt the chemisorption of water molecules on the cluster.

It is not only the Al100 cluster case in which the water molecule obstructing its own reaction is observed. The same water self poisoning phenomenon is observed for Al200 cluster. As shown in Figure **3-12**, although the number of adsorbed water molecules increases with the number of water molecules initially added in the gas phase, the more adsorbed water molecules don't necessarily dissociate more during the reaction, which is shown in Figure **3-13**, Figure **3-14** and Figure **3-15**. As a matter of fact, the excessive water molecules hinder both the chemisorption and dissociation process, and result in the reduction of hydrogen evolution from the reaction, shown in Figure **3-16**.

3.1.6 Water Molecule Conversion Rate

So far, the influences of water assistance and water self poisoning are discussed in aluminum-water reaction. In order to promote the reaction for hydrogen generation and at the same time make the most efficient use of reactants, it is crucial to control the amount of water molecules used in the reaction. Therefore, a water molecule conversion rate is defined as the ratio of the number of water molecules dissociated $\boldsymbol{N}_{\boldsymbol{H_2O,dis}}$ during the reaction to the total number of water molecules $\boldsymbol{N}_{\boldsymbol{H_2O,i}}$ added initially into the system, to present the efficiency of water usage.

$$\boldsymbol{\alpha}_{\boldsymbol{H_2O}} = \boldsymbol{N}_{\boldsymbol{H_2O,dis}} \big/ \boldsymbol{N}_{\boldsymbol{H_2O,i}} \tag{3.6}$$

Figure **3-17** shows the variation of dissociation percentage of water molecules when different amount of water molecules are added initially into the Al100 reaction system. The conversion rate first increases with the number of water molecules because of the water reaction assistance effect; and then decreases with the number of water molecules due to the water self poisoning effect. When only 10 water molecules are initially added into the system, none of them are dissociated, and when 100 water molecules are added, most of the water molecules are

adsorbed to Al cluster but only a few, 13%, are dissociated because of water self poisoning. Water molecules completely dissociate when 30 water molecules are added originally. Although higher water molecule conversion rate does not directly relate to higher hydrogen production, it does provide a clearer idea about the efficiency of water usage and the potential of possible hydrogen generation.

3.1.7 Influence of Temperature on Water Adsorption and Dissociation

Temperature is one of the most important parameters that affect reactions. In this work, temperature influences on aluminum-water reaction are studied by altering the temperature of Al cluster. As described in Chapter 2, temperatures of Al cluster, water molecules as well as Neon atoms are controlled in the simulation using an optional ReaxFF file called 'tregime.in', which is used to define the initial and final temperature of the reactants, heating rate, heating up or cooling down time step, and temperature damping constant. In the basic cases, the aluminum cluster is kept at $0K$ at all times. The water molecules first enter the system at $0K$, then they are heated up eventually at a heating rate of $0.005K$ per time step, the final temperature of water molecule is $1650K$. For the cases in which Neon atoms are also involved, the initial temperature of Neon atom is also $0K$, after being heated up using the same heating rate as that of water molecule, the final temperature of Neon atoms is $1650K$ as well. In order to evaluate the temperature influence, the initial temperatures of both Al cluster and water molecules are raised to $300K$. The same heating rate is applied. Table **3-1** summarizes the temperature control profile specified in 'tregime.in' file.

Figure **3-18**, **3-19**, and **3-20** show the intermediate species generated during the reaction for each of the three cases. By increasing the initial temperature of Al cluster and water molecules, reaction kinetics are enhanced. The number of broken OH bonds in Case 2 is the most, which is shown in Figure **3-21**. More broken OH bonds resulted in less adsorbed hydroxyl (Figure **3-18**) and more adsorbed hydrogen (Figure **3-19**) and oxygen (Figure **3-20**) on Al cluster. At elevated temperature, reaction kinetics is enhanced, which results in an increase of the possible reaction pathways and facilitating the production of intermediate species. Table **3-2** summarizes the molecular compositions at the end of each simulation.

3.1.8 Temperature Distribution of Aluminum Cluster

During the simulations, aluminum cluster is kept at a low temperature, while heating up water molecules and Neon atoms (if added) eventually. Figure **3-22** shows a typical temperature distribution of the aluminum atoms of the aluminum cluster at the end of simulation. A majority of the 100 aluminum atoms maintain a relatively low temperature during the reaction and only very few aluminum atoms reach a higher temperature. This temperature distribution proves the temperature controlling steps applied for the simulations are reasonable and feasible.

3.2 Influence of Noble Gas on Aluminum/Water Reaction

In order to control the water molecule concentration and water reaction rate, non-reacting noble gas Neon is added into the Al water reaction system in this study, acting like inert water.

3.2.1 Behavior of Noble Gas Neon in the System

Since Neon dose not react with any species in the system, the interactions between Neon atoms and Al cluster and adsorbed water molecules are the main focus. Figure **3-23** captures how Neon atom collides with Al cluster. There are temporary chemisorptions of Neon atoms on Al cluster followed by desorption process.

The interactions between Neon atoms and adsorbed water molecules are shown in Figure **3-24**, in which the direct collision of Neon atoms with adsorbed water molecules is not observed. For a Neon atom to collide with adsorbed water molecules, it has to overcome the intermolecular repulsion between itself and water molecules. If the energy adsorbed by Neon atoms from the reaction system can not balance the energy required to overcome the work needed to be done due to intermolecular repulsion, Neon atoms can not collide with adsorbed water molecules.

3.2.2 Influence of Noble Gas Concentration on Water Adsorption and Dissociation

The temperature controlling steps for Al cluster, water molecules, and Neon atoms are listed in Table **3-3**. For this set of simulations, Al cluster is kept at $0K$ during the simulation, and water molecules and Neon atoms are heated at the same heating rate for the same amount of heating time. The Neon gas concentration C_{Ne} is defined as the ratio of the number of Neon atoms N_{Ne} to the total number of Neon atoms and water molecules. Similarly, the water concentration is defined as the ratio of the number of water molecules N_{H_2O} to the total number of water molecules and neon atoms, which are shown below:

$$C_{H_2O} = N_{H_2O} \Big/ \left(N_{Ne} + N_{H_2O} \right) \tag{3.7}$$

$$C_{Ne} = N_{Ne} \Big/ \left(N_{Ne} + N_{H_2O} \right) \tag{3.8}$$

Figure **3-25** describes the variation of the number of broken OH bonds for all five cases. When Neon atoms are present in the system, they adsorb some energy from the reaction. In Case 5, no Neon gas is added into the system, then more energy can be used to break OH bond, resulting in a higher water molecule conversion rate. So the number of broken OH bonds deceases with the number of Neon atoms added. The adsorbed hydroxyl and oxygen atom on the Al cluster are directly related to the breaking of OH bonds. This explains why the number of adsorbed hydroxyl and adsorbed oxygen atoms are also the most in Case 5, which is shown Figure **3-26** and Figure **3-27**. Actually, shown in Figure **3-27**, no adsorbed oxygen atoms are observed in Case 1 and Case 2, in which a lot of Neon gas is added resulting in less energy left for breaking the OH bonds.

The number of adsorbed water molecules depends both on the initial chemisorption of water molecule on the cluster and the subsequent dissociation process. Figure **3-28** shows the variation of number of adsorbed water molecules for different Ne gas concentration (related to different water molecule concentration) cases. For Case1, in which the Neon gas concentration is 50%, 46 out of 50 water molecules are adsorbed to the cluster without dissociation at the end of the simulation; the water molecule conversion rate is as low as 8%. As discussed earlier, Neon atoms prevent the water molecules from connecting with each other, by bouncing around in the reaction system, and thus prohibit the formation of water molecule layers around Al cluster. This actually protects the available reaction sites on the cluster from being covered by water molecule layer. Subsequently, the chemisorption of water molecules to the Al cluster is easier. On the other

hand, when more Neon atoms are present in the system, less energy is left for the dissociation of water molecules. It is observed that when Neon gas concentration is 50%, the chemisorption of water molecule is promoted while the dissociation of water molecule is prohibited. Therefore, the number of adsorbed water molecules for Case 5 is the most. Table **3-4** summarizes the molecular compositions as well as the change of potential energy at the end of each simulation.

3.3 Aluminum Particle Size

The use of nano-sized particles (Aln) in the aluminum-water reaction can offer significant advantages over larger size particles. Much of the highly desirable traits of nano-sized metal powders in combustion systems can be attributed to their high specific surface area (high reactivity) and overall small dimensions (short reaction times). Aln particles have the ability to absorb large amounts of water on the surface as well as to heat up quicker (smaller heat capacity) [58].

Understanding how a specific shape or size will affect the reactivity of aluminum cluster toward water molecules may facilitate future efforts to design either stable or reactive materials for specific technological applications like fuel cells. In this work, at nano-scale, the important role of aluminum cluster size playing in determining the reactivity of aluminum-water reaction is studied.

The nano-sized aluminum particles studied are Al100 and Al200 clusters. For each cluster, the aluminum-water reaction is studied at three different water concentrations, 50%, 75% and 100%. As discussed earlier, the number of water molecules added is determined in such a way that the average surface coverage of Al cluster by water molecules is maintained the same for different Al clusters. Therefore, the only reason that accounts for the differences in the reactivity of Al cluster with water is the geometric structure or the size of the metal cluster. The temperature control for the each of the reactants is listed in Table **3-5** and **3-6**.

3.3.1 Influence of Aluminum Particle Size on Water Dissociation Rate

Figure **3-29** shows the variation of the number of broken OH bonds under different water concentrations for Al100 cluster and Al200 cluster. Figure **3-30**, **3-31**, and **3-32** present the

variation of the number of broken OH bonds for both Al100 and Al200 clusters under the same initial water concentration. As the reaction proceeds, the number of broken OH bonds increases. For Al100 cluster, there are roughly about 50-60 sites available for surface reaction. Obviously, more available surface reaction sites are provided by Al200 cluster. As a result, the dissociation of water molecules is made more possible because more available surface sites are provided for the dissociated atoms to move into.

The most broken OH bonds are generated in the case of Al200 cluster, when initial water concentration is 75%. When the water concentration is 50%, the size of Al cluster does not have a huge influence on the number of broken OH bonds. This might be caused by the Ne atoms added for the Al200 case adsorbing a large amount of thermal energy from the reaction or the dissociative chemisorption, leaving the reactants and also intermediate species containing less thermal energy for the dissociation process. In general, under the same average surface water molecule coverage for Al cluster, the number of broken OH bonds which represents the water conversion rate (or water dissociation rate) increases with the Al cluster size.

3.3.2 Optimum Water Concentration for Al100 and Al200

When Neon gas is applied as inert water, the reactivity of Al cluster with water is influenced by the number of Neon atoms added for Al100 cluster which is discussed earlier. For Al200 cluster, the reactivity of aluminum-water reaction is also affected by water concentration (or Neon concentration). Figure **3-33** shows the variation of the number of broken OH bonds, which represents the water dissociation rate during the reaction for Al 100 cluster, while Figure **3-34** shows the same parameters for Al 200 cluster. Similarly, for both Al100 and Al200 clusters, a value of 75% water concentration helps achieve a better water conversion rate.

This phenomenon can be explained by the effects of adding Ne gas. Applying Neon atoms prevents water molecules self poisoning, which is caused by the water molecule layers around the Al cluster which covers the available surface reaction sites and blocks the pathway of reactants and intermediate species to arrive at the Al cluster. Therefore, certain amount of Ne atoms is needed to be present in the system to inhibit water molecule self poisoning, but not too much because of the energy adsorption of Ne gas from the system. According the simulation results, an optimum water concentration, which is 75%, is observed under which the highest water dissociation rate is achieved for both Al100 and Al200 clusters.

3.4 Aluminum Oxide Layer

Due to the strong affinity for oxygen, aluminum and its alloys are usually well protected by a thin coherent, adhering layer of aluminum oxide. This aluminum oxide layer prevents the spontaneous reaction of aluminum with water. A considerable amount of research is focusing on approaches of promoting aluminum-water reaction by either chemical, mechanical activation method or both of them, based on the idea of continual removal and disruption of the aluminum oxide layer [23-37, 44-47]. In this work, by integrating ReaxFF with molecular dynamic modeling, the fundamental mechanisms of aluminum oxide layer influences on aluminum-water reaction is investigated at a molecular level.

3.4.1 Influence of Aluminum Oxide Layer on Water Adsorption to Aluminum Cluster

Table **3-7** lists the temperature controlling steps for the cases discussed for this analysis. The Al cluster, or the Al cluster with aluminum oxide layer is kept at a low temperature of $0K$, and the heated water molecules are added into the system. For Case 2, 3 and 4, Figure **3-35**, **3-36**, and **3-37** show the formation of aluminum oxide layer on aluminum cluster

The variation of the number of adsorbed water molecules on Al cluster for each case is described in Figure **3-38**. Initially, the adsorption of water molecules onto the Al cluster is the dominating event, so the number of adsorbed water molecules increases with time initially, no matter whether the aluminum oxide layer is present in the system or not. Subsequently, the dissociation of adsorbed water molecules takes place while the chemisorption proceeds. The number of adsorbed water molecules decreases later in the reaction for the case (Al100_H_2O50) in which there is no aluminum oxide layer developed on the Al cluster. The dissociation easily proceeds in this case because the surface sites are not covered and are available for intermediate species to move into.

However, for the cases in which aluminum oxide layer is formed on the surface of Al cluster, the number of available surface sites for reaction is reduced. As a result; the adsorption of water molecules to the clusters is hindered, followed by an also prohibited dissociation process. It is observed from Figure **3-38**, the number of adsorbed water molecules on the Al cluster in cases, where aluminum oxide layer is formed is much less than that of the case in which no aluminum oxide layer is formed. Due to the fact that the dissociation process is also suppressed because of

the loss of the available surface sites, the number of adsorbed water molecules in Case 2, 3 and 4 dose not decrease prominently later in the reaction. As a matter of fact, when the aluminum oxide layer is thick enough, as in Case 4, few surface sites are available for water molecules to adsorb to the Al cluster.

3.4.2 Influence of Aluminum Oxide Layer on Water Dissociation Rate

Figure **3-39** shows the variation of the number of adsorbed OH bonds on Al cluster for each case. When no aluminum oxide layer is formed on the cluster surface, initially, there is no adsorbed hydroxyl on the Al cluster. After a certain period of time, the dissociation of adsorbed water molecules process proceeds, an increase in the number of adsorbed hydroxyl on the cluster later in the reaction is observed in Case 1.

For Cases 2, 3 and 4, where an aluminum oxide layer is present on the surface of cluster, the adsorbed water molecules begin to dissociate at an earlier stage in the reaction. As the reaction proceeds, the number of adsorbed hydroxyl on the cluster increases. Similarly, the thicker the aluminum oxide layer is, the less the adsorbed hydroxyl on the cluster. The variation of adsorbed hydrogen atom on the Al cluster is described in Figure **3-40**. The formation of adsorbed hydrogen atoms on the Al cluster followed the initial chemisorption and subsequent dissociation of water molecules. As reaction continues, more adsorbed hydrogen atoms are observed.

Table **3-8** summarized the molecular composition of the system at the end of Aluminum-Water reaction. The existence of aluminum oxide layer prevents the chemisorption and dissociation of water molecules. As the aluminum oxide layer becomes thicker, aluminum-water reaction is more suppressed, which is demonstrated in Table **3-8** by the fact that more water molecules are left un-reacted in the gas phase and fewer intermediate species are produced.

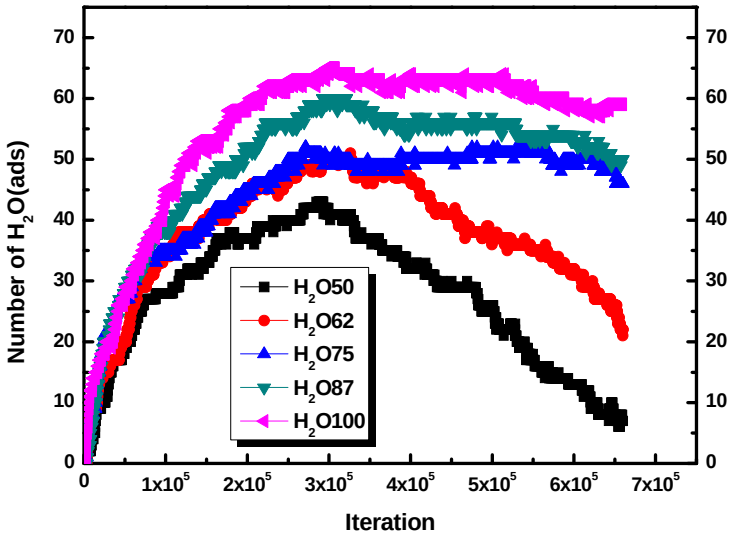

Figure **3-1**: Profile of variations of adsorbed water molecules on Al100 cluster versus iteration steps under different water molecules added into the Al100 system

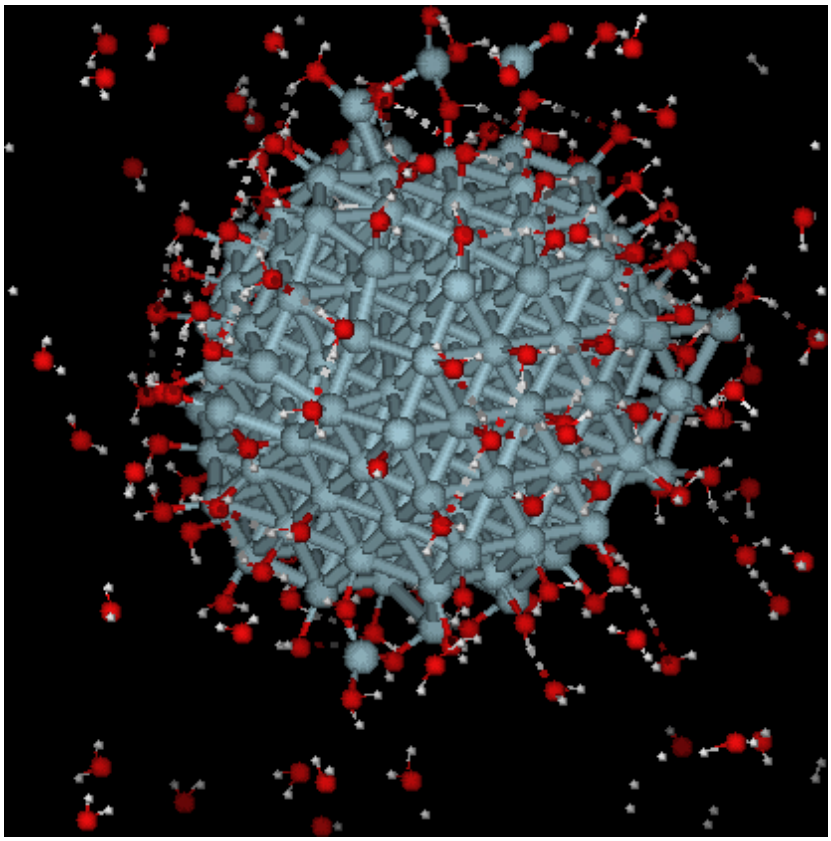

Figure **3-2**: Snapshot of Al cluster and water molecules during the reaction
(Gray: Al atoms, Red: oxygen atoms, White: hydrogen atoms)

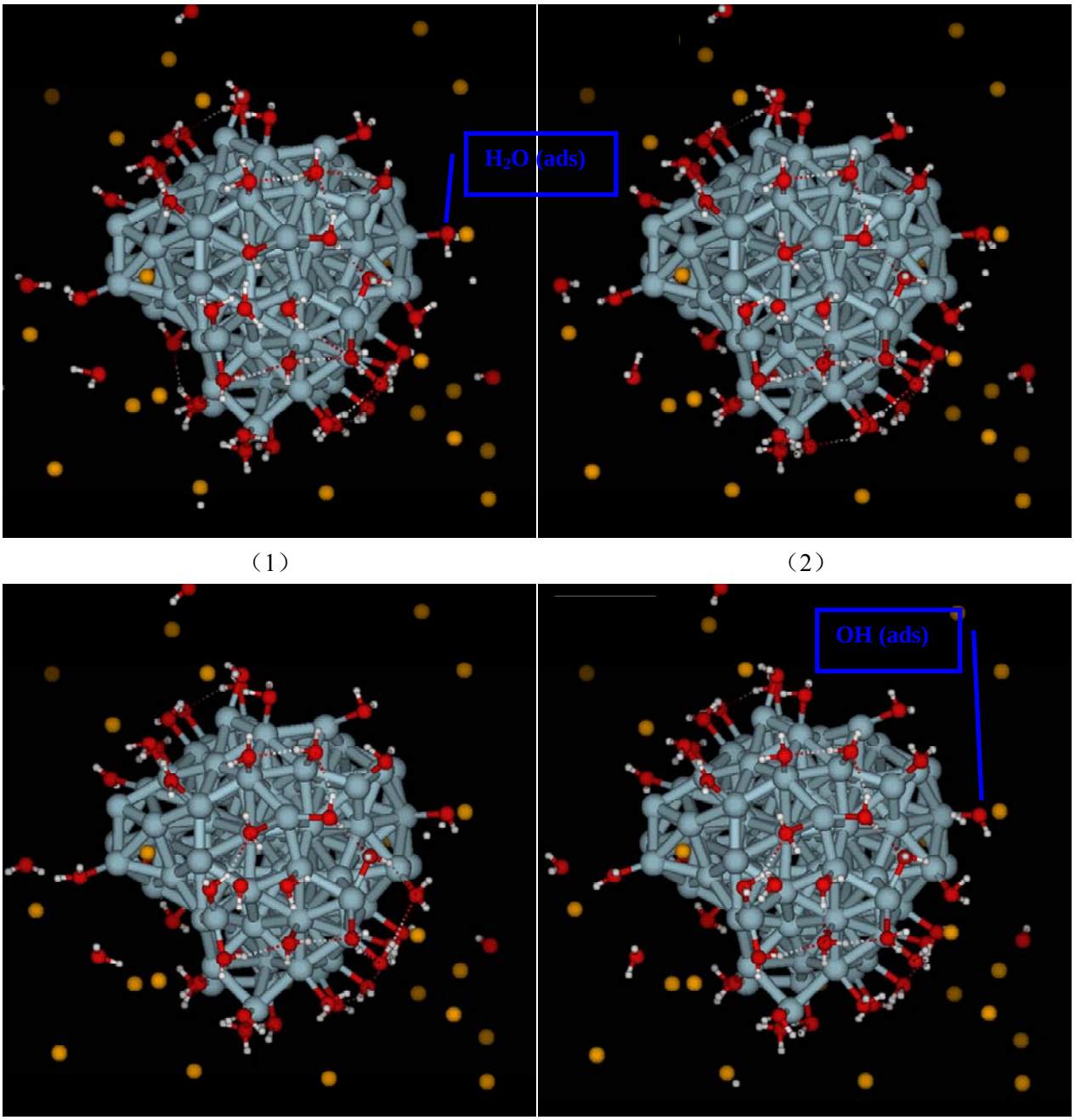

Figure **3-3**: Snapshots of dissociation process of adsorbed water molecule (Gray: Al atoms, Red: oxygen atoms, White: hydrogen atoms, Yellow: Neon atoms)

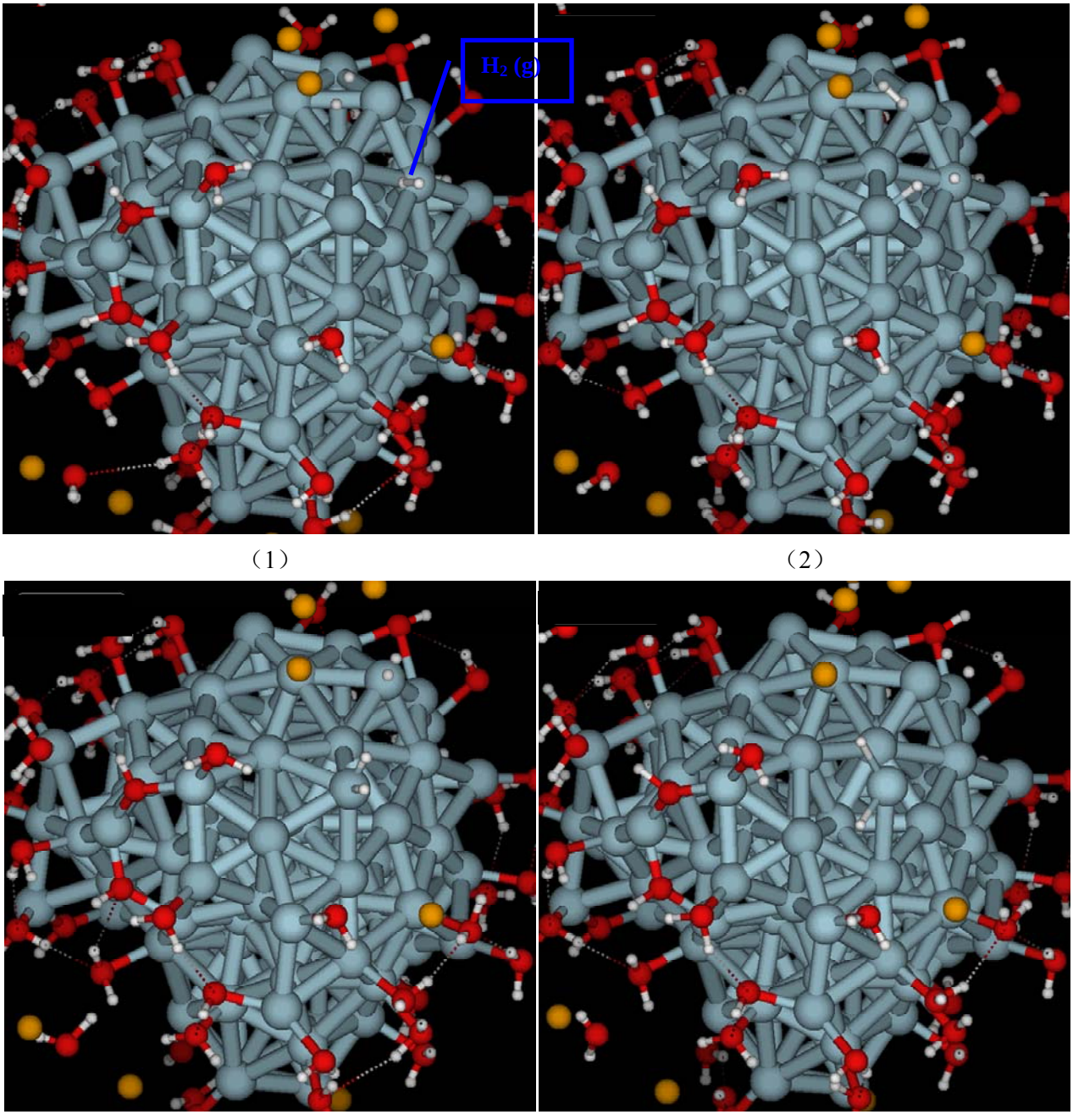

Figure **3-4**: Snapshots of formation of adsorbed hydrogen atom on Al cluster (Gray: Al atoms, Red: oxygen atoms, White: hydrogen atoms, Yellow: Neon atoms)

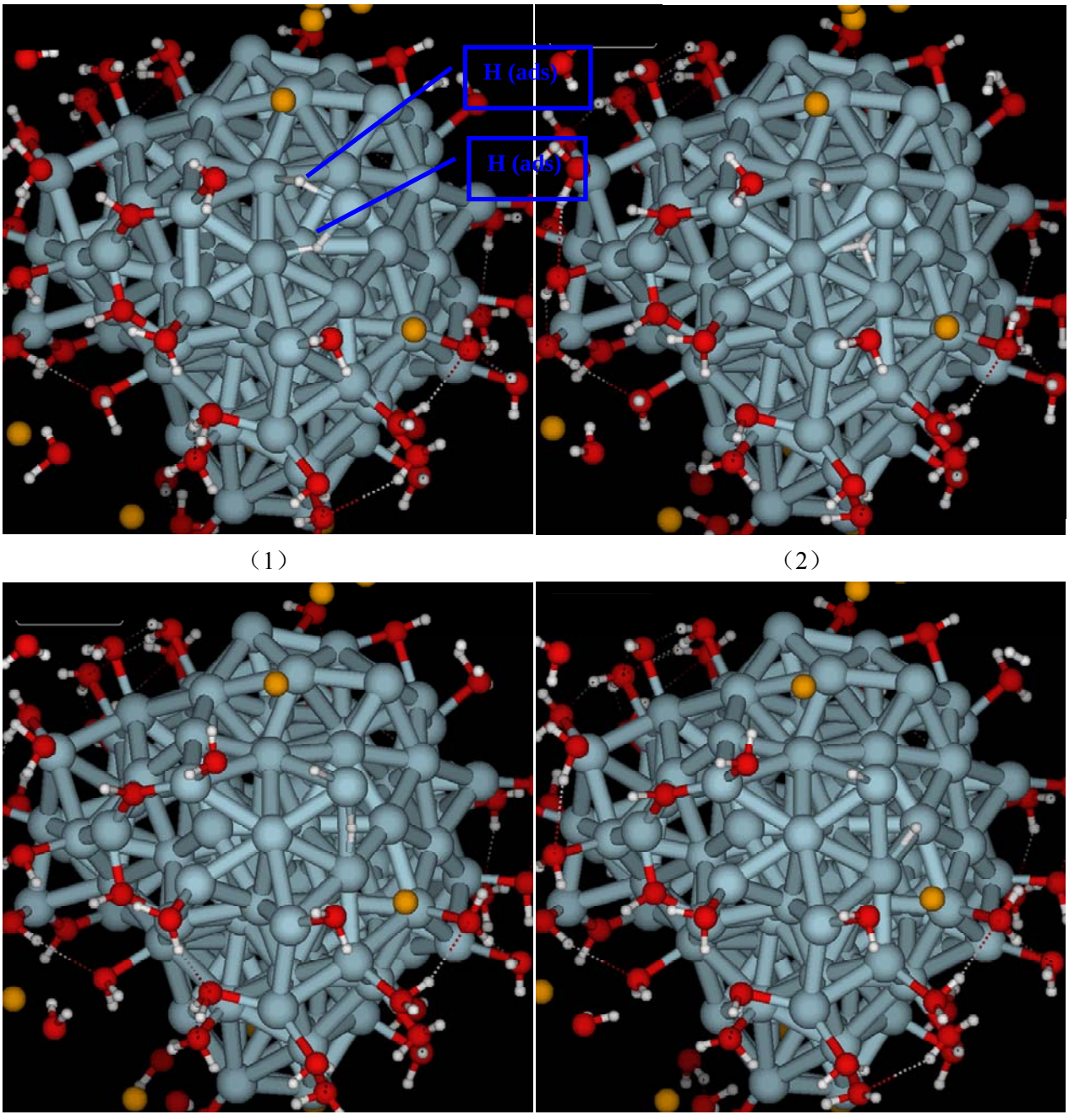

Figure **3-5**: Snapshots of adsorbed hydrogen atoms on Al cluster (Gray: Al atoms, Red: oxygen atoms, White: hydrogen atoms, Yellow: Neon atoms)

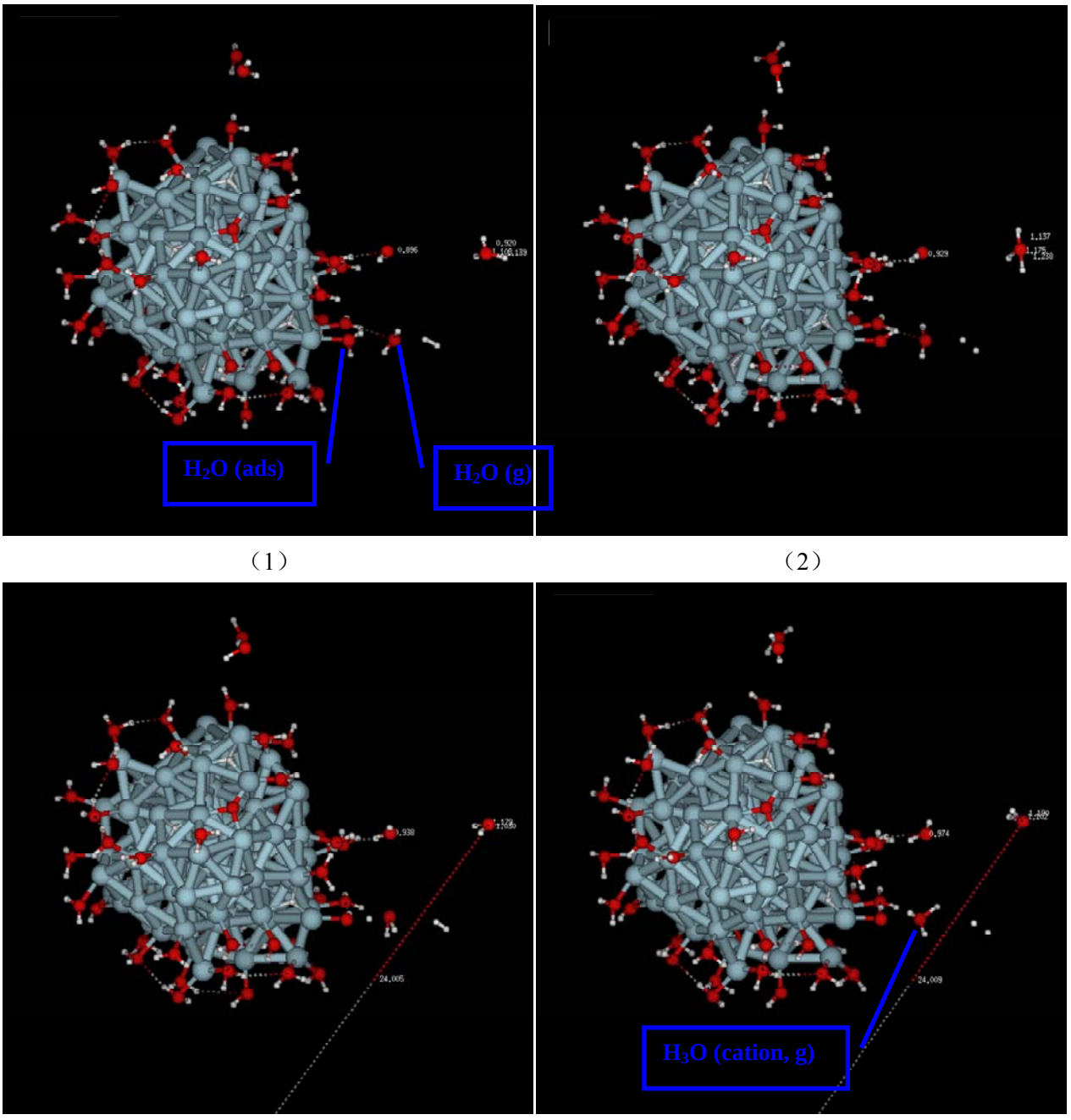

（1） （2）

（3） （4）

Figure **3-6**: Snapshots of formation of hydronium ion H_3O (cation, g) in the gas phase (Gray: Al atoms, Red: oxygen atoms, White: hydrogen atoms)

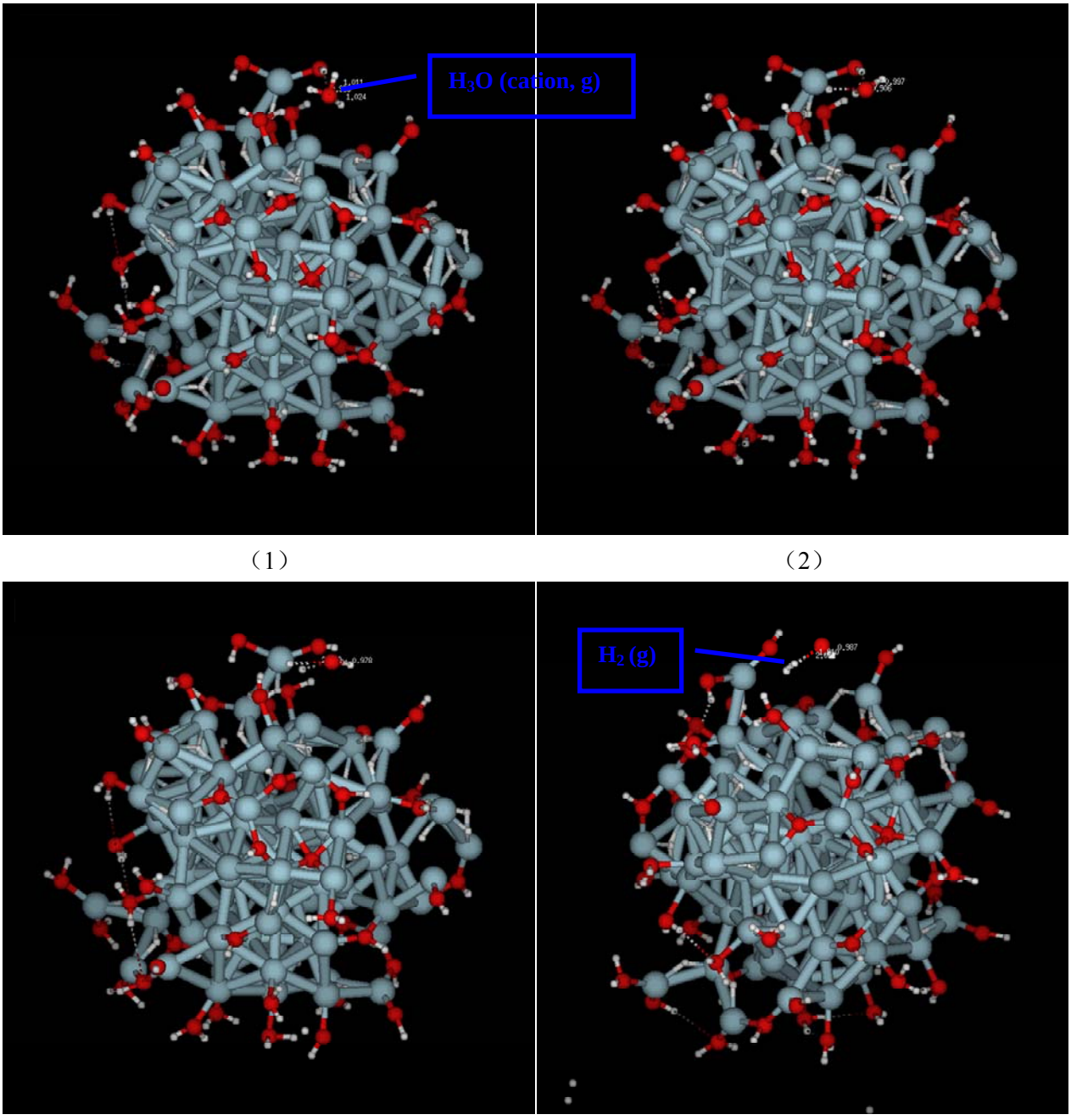

（1） （2）

（3） （4）

Figure **3-7**: Snapshots of surface reaction involving hydronium ion H_3O (cation, g)- hydrogen generation (Gray: Al atoms, Red: oxygen atoms, White: hydrogen atoms)

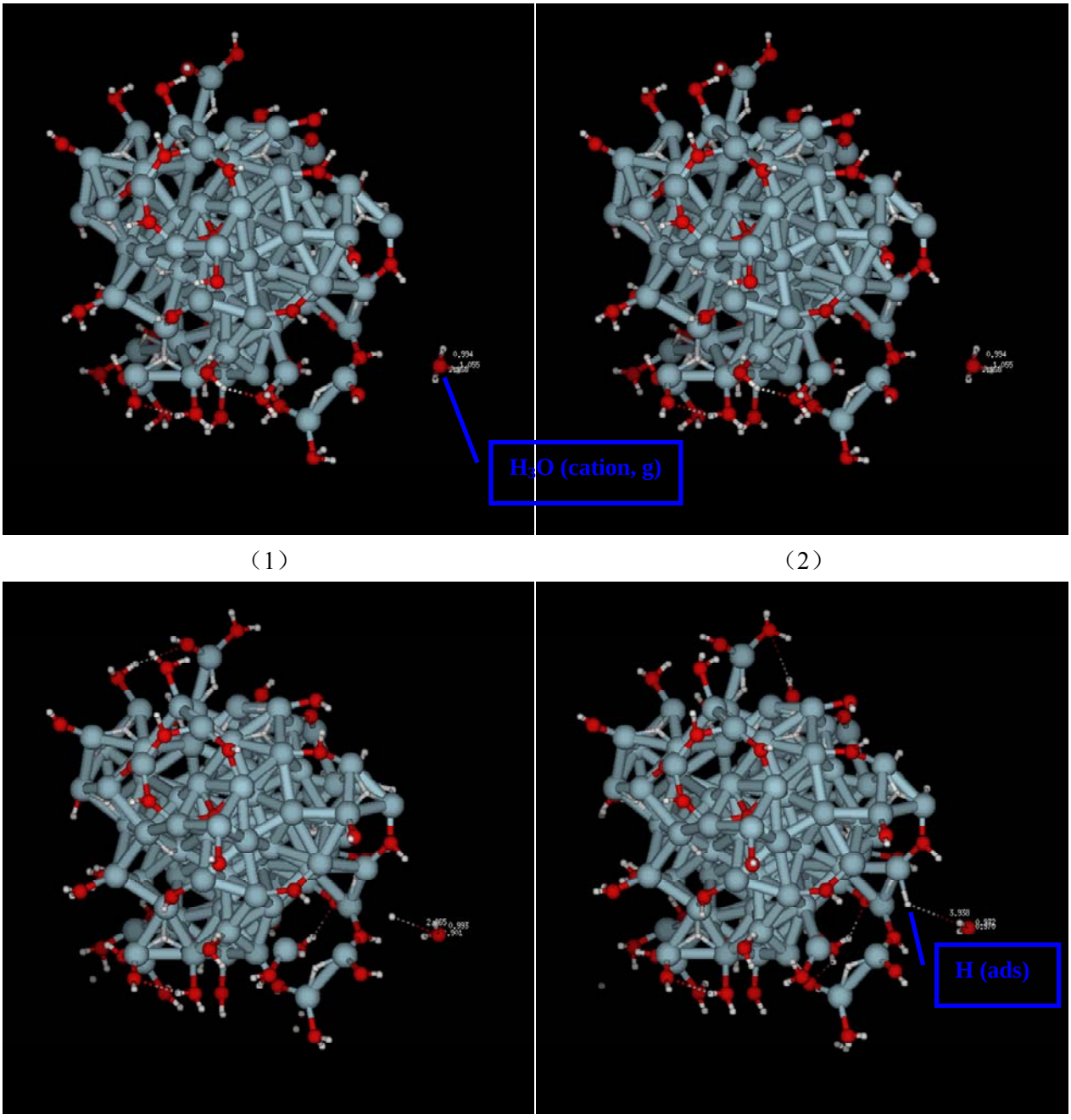

（1） （2）

（3） （4）

Figure **3-8**: Snapshots of surface reactions involving hydronium ion H_3O (cation, g)- Al-H bond formation (Gray: Al atoms, Red: oxygen atoms, White: hydrogen atoms)

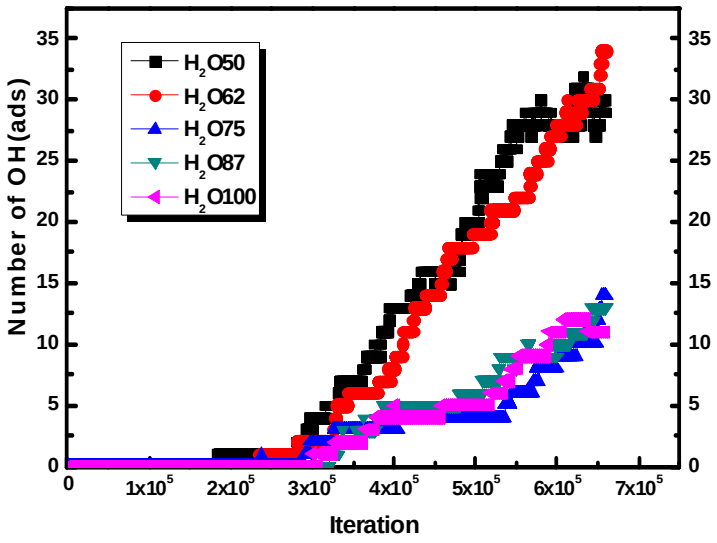

Figure **3-9**: Profile of variations of adsorbed hydroxyl on Al100 cluster versus iteration steps under different water molecules added into the Al100 system

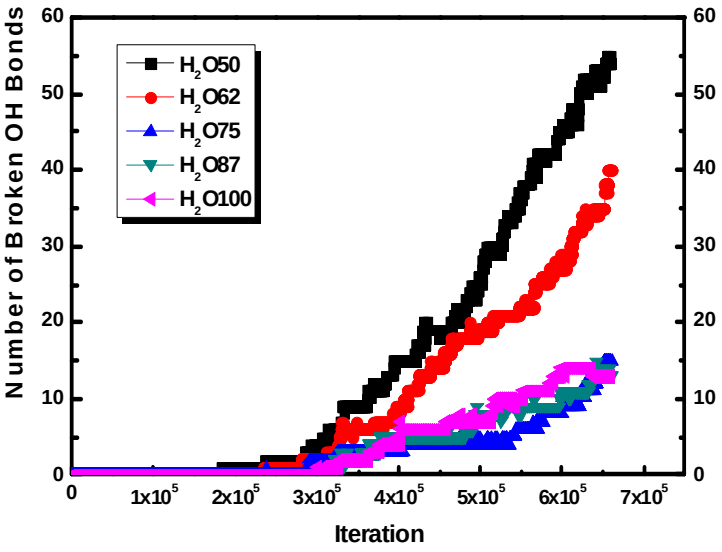

Figure **3-10**: Profile of variations of broken OH bonds versus iteration steps under different water molecules added into the Al100 system

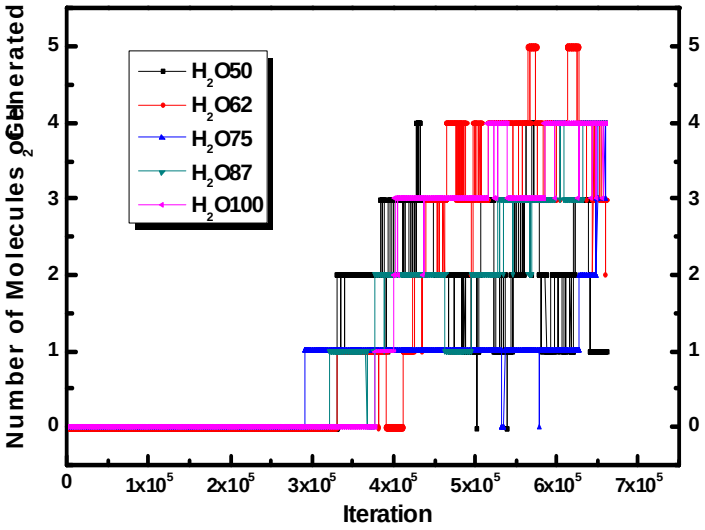

Figure **3-11**: Profile of variations of hydrogen generation versus iteration steps under different water molecules added into the Al100 system

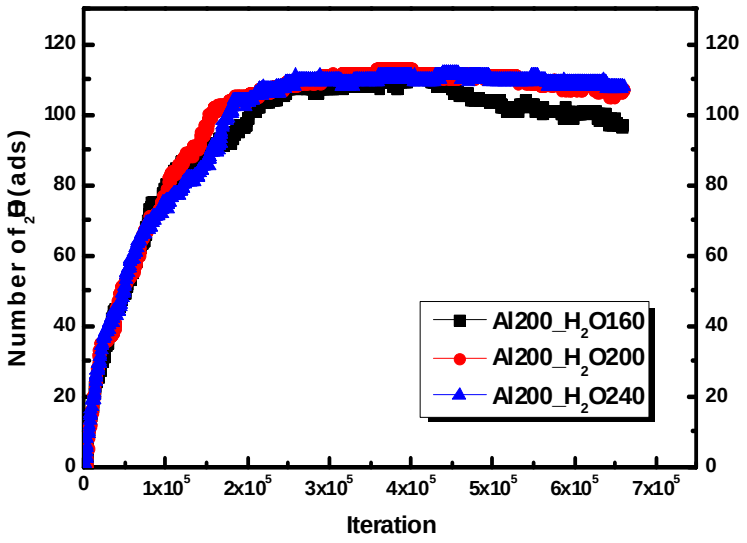

Figure **3-12**: Profile of variations of adsorbed water molecules on Al200 cluster versus iteration steps under different water molecules added into the Al200 system

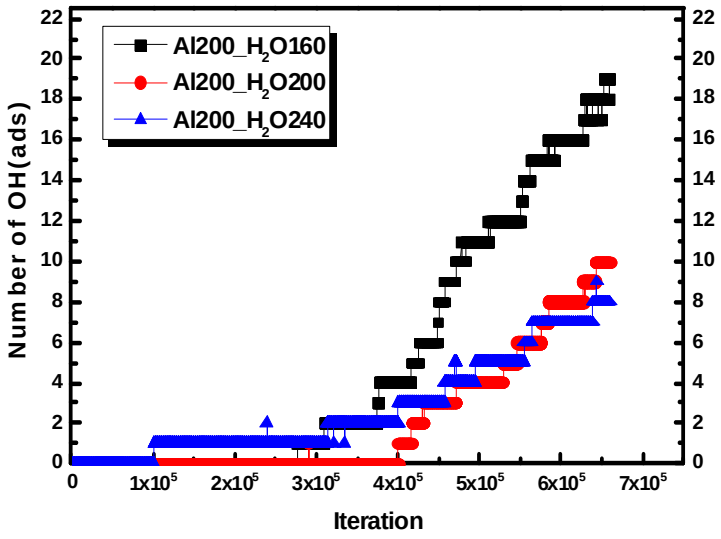

Figure **3-13**: Profile of variations of adsorbed hydroxyl on Al200 cluster versus iteration steps under different water molecules added into the Al200 system

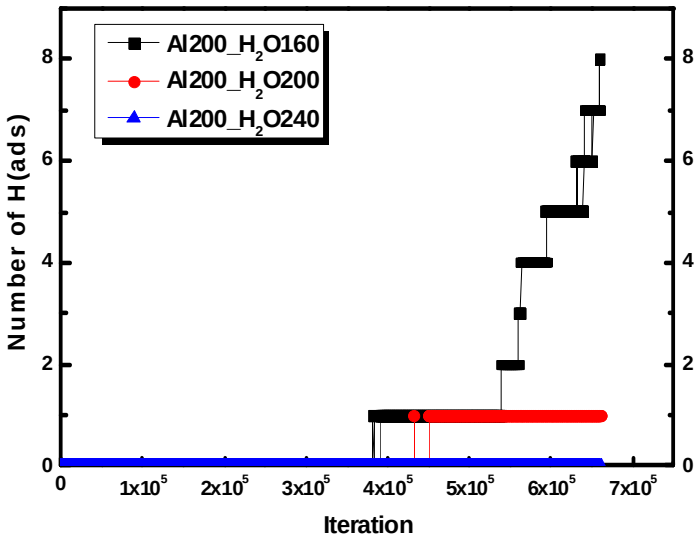

Figure **3-14**: Profile of variations of adsorbed hydrogen atoms versus iteration steps under different water molecules added into the Al200 system

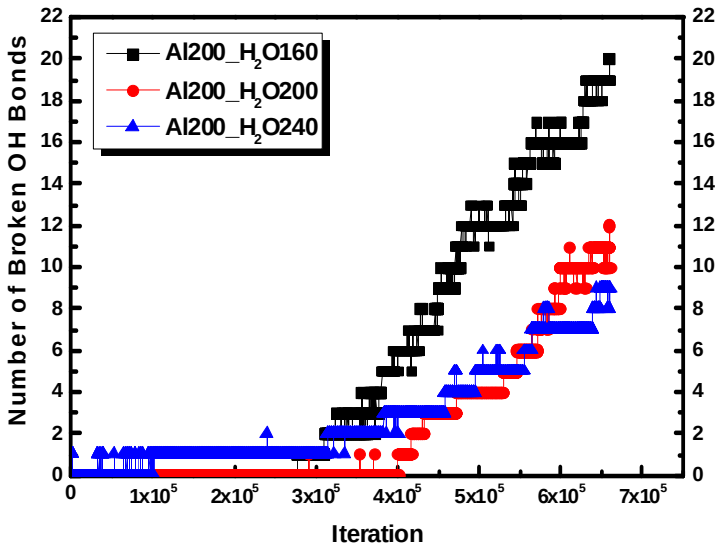

Figure **3-15**: Profile of variations of broken OH bonds versus iteration steps under different water molecules added into the Al200 system

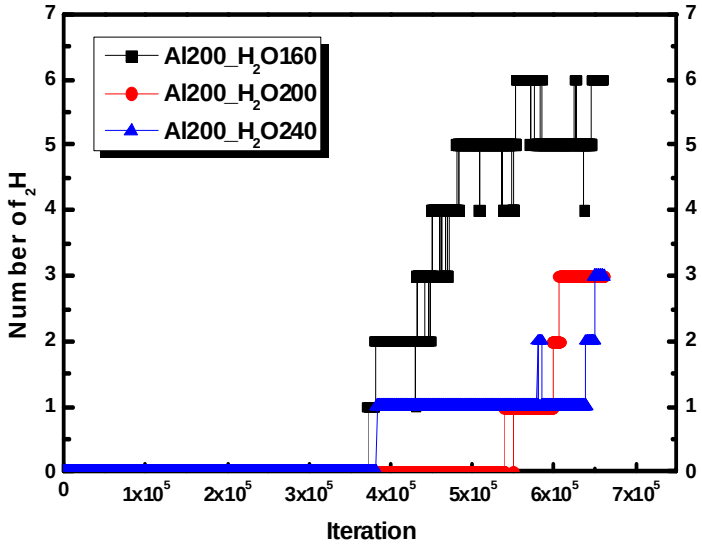

Figure **3-16**: Profile of variations of hydrogen generation versus iteration steps under different water molecules added into the Al200 system

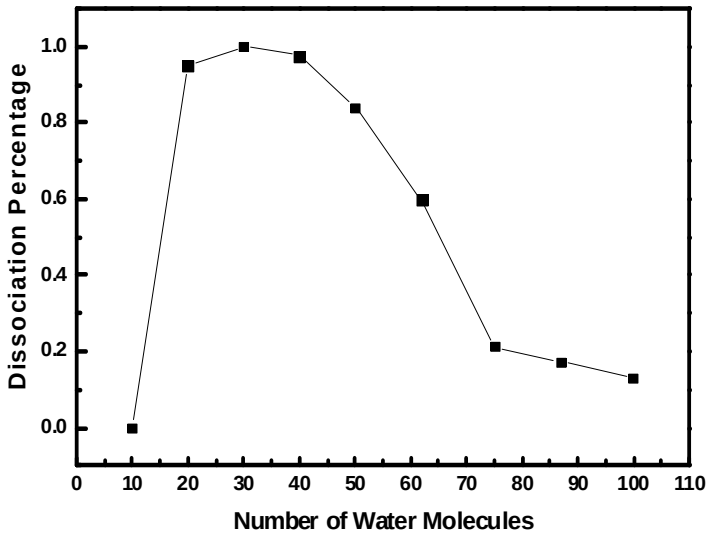

Figure **3-17**: Variations of water molecule conversion rate at the end of the reaction versus number of water molecules added initially into the Al100 system

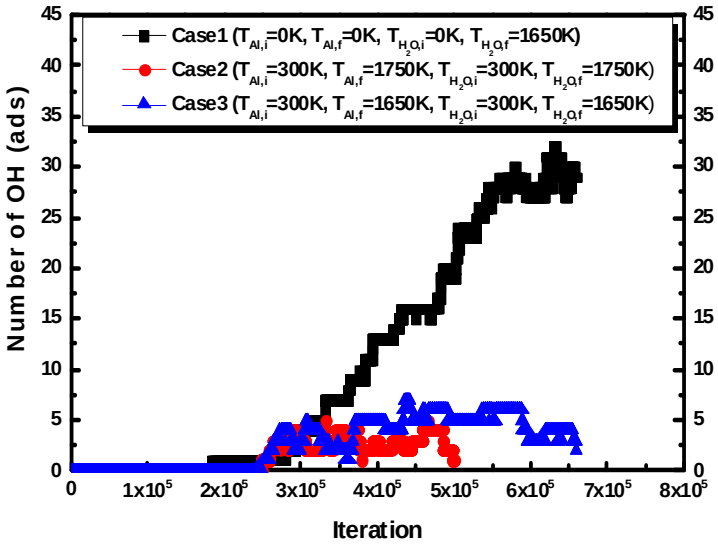

Figure **3-18**: Variation of the number of adsorbed hydroxyl on Al cluster for different temperature control cases

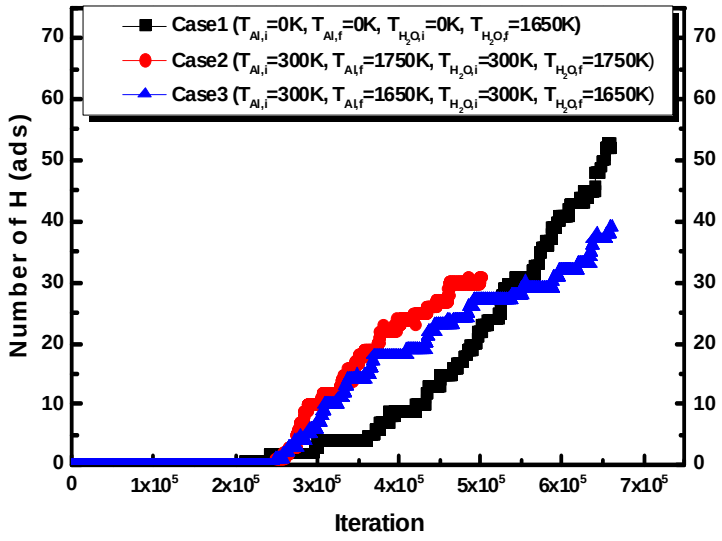

Figure **3-19**: Variation of the number of adsorbed hydrogen on Al cluster for different temperature control cases

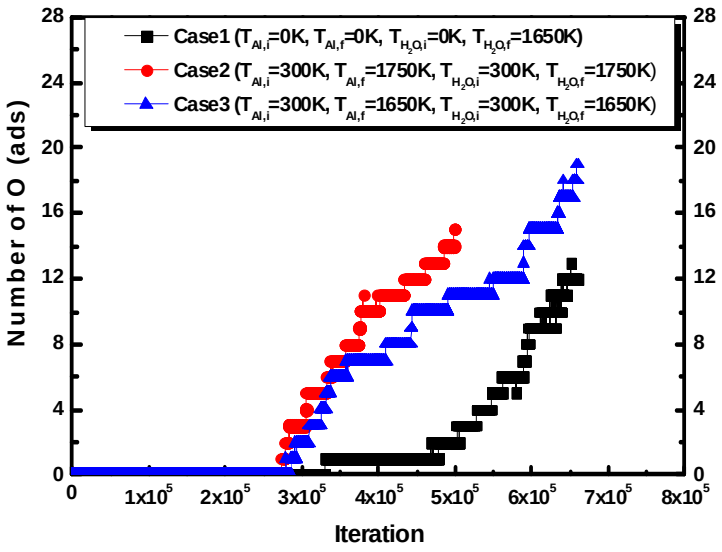

Figure **3-20**: Variation of the number of adsorbed oxygen on Al cluster for different temperature control cases

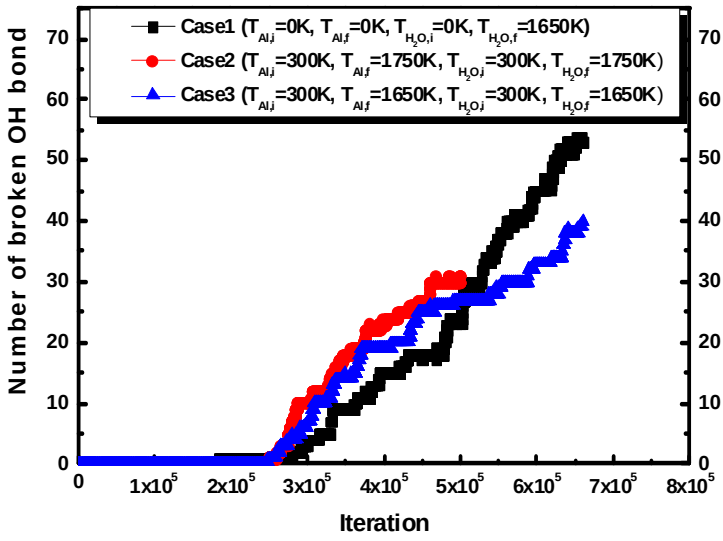

Figure **3-21**: Variation of the number of broken OH bonds for different temperature control cases

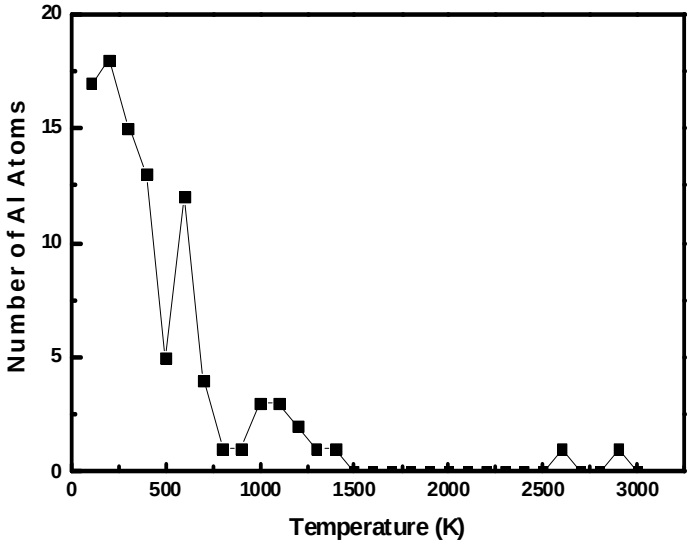

Figure **3-22**: Temperature distribution of aluminum atoms of Al100 cluster at the end of simulation

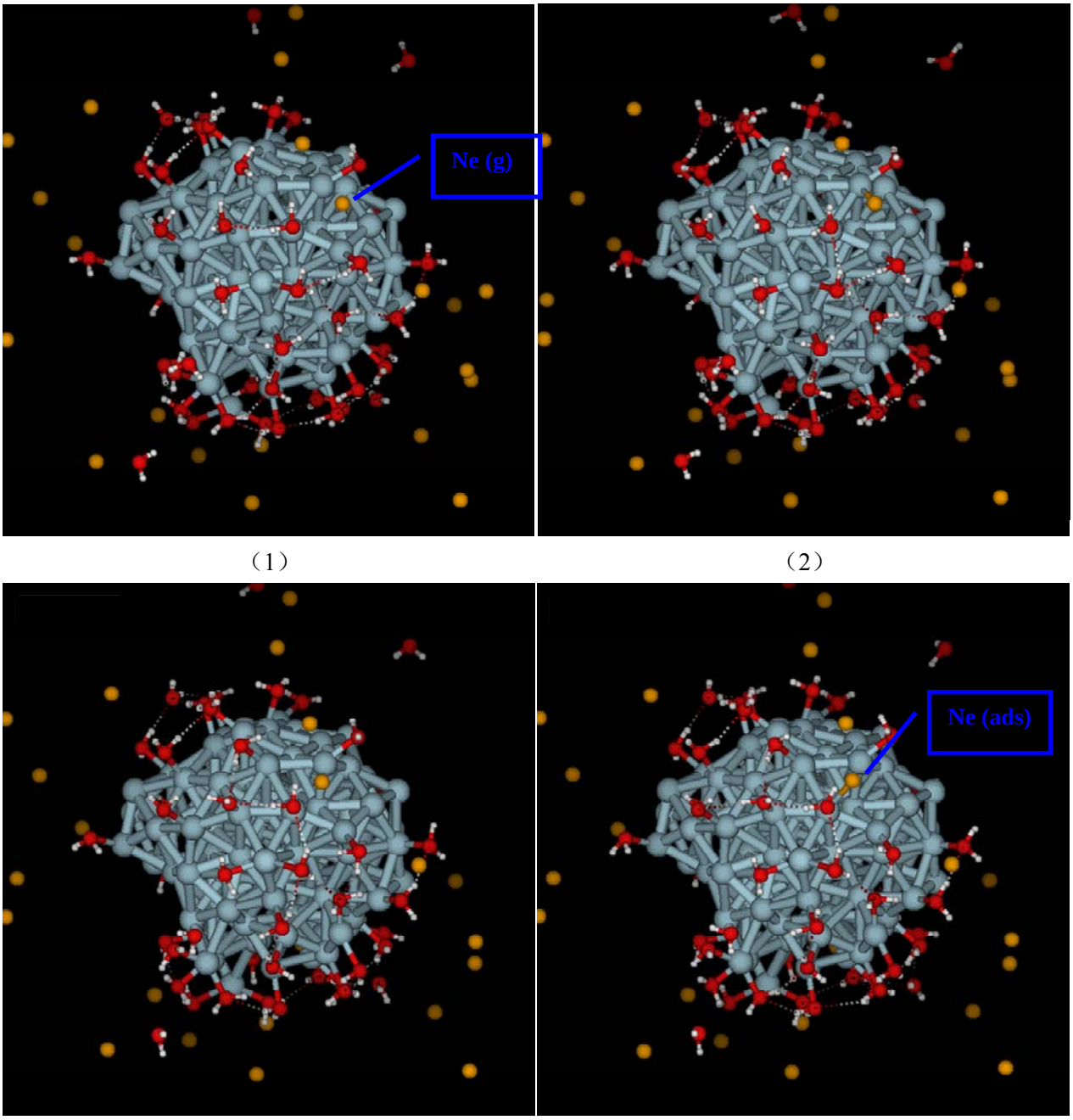

（1） （2）

（3） （4）

Figure **3-23**: Snapshots of interactions between Neon atoms and Al cluster (Gray: Al atoms, Red: oxygen atoms, White: hydrogen atoms, Yellow: Neon atoms)

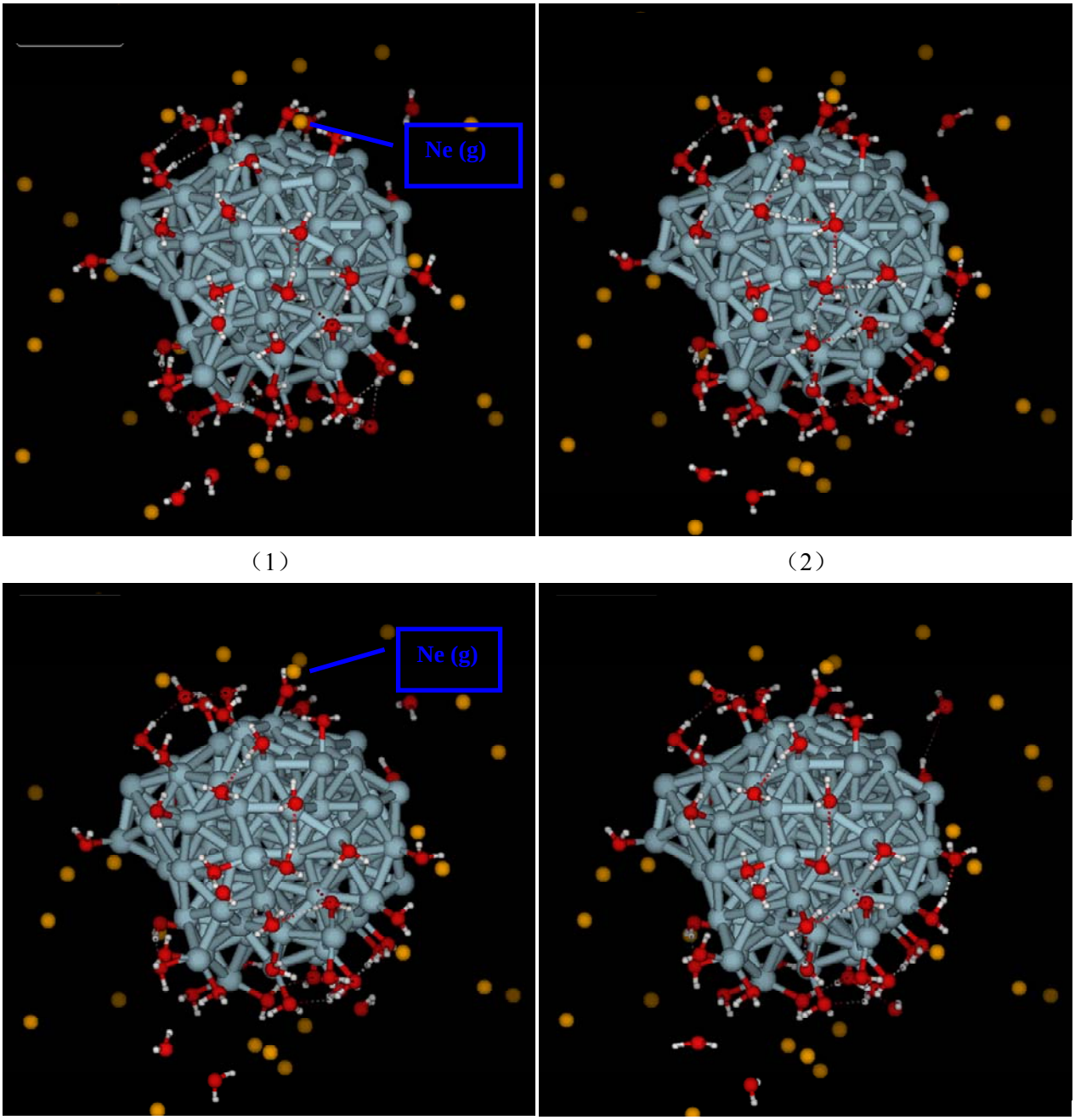

（1） （2）

（3） （4）

Figure **3-24** Snapshots of interactions between Neon atoms and adsorbed water molecule (Gray: Al atoms, Red: oxygen atoms, White: hydrogen atoms, Yellow: Neon atoms)

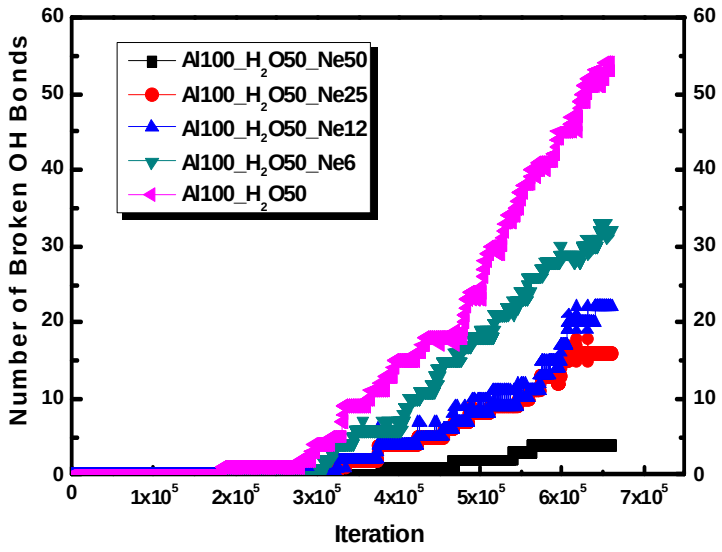

Figure **3-25**: Variation of the number of broken OH bonds for different Ne gas concentration cases

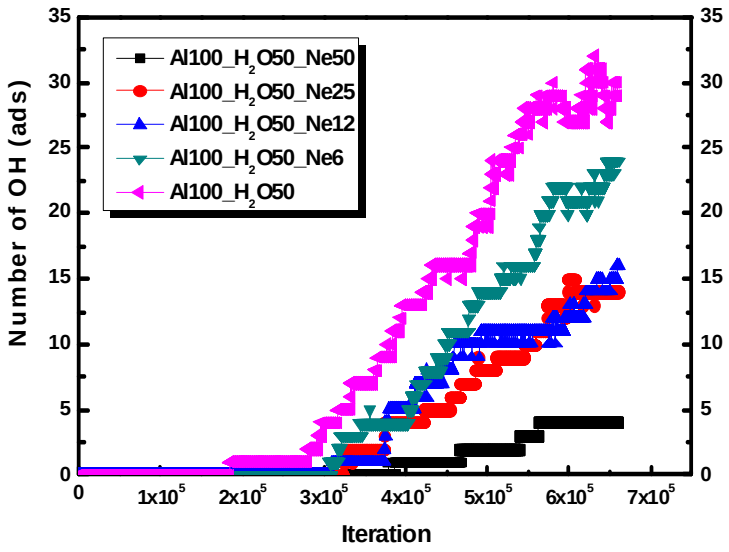

Figure **3-26**: Variation of the number of adsorbed hydroxyl on Al cluster for different Ne gas concentration cases

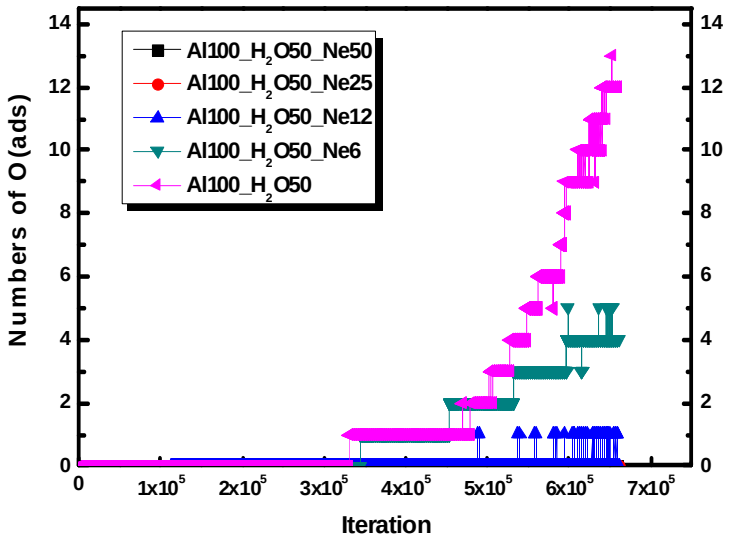

Figure **3-27**: Variation of the number of adsorbed oxygen on Al cluster for different Ne gas concentration cases

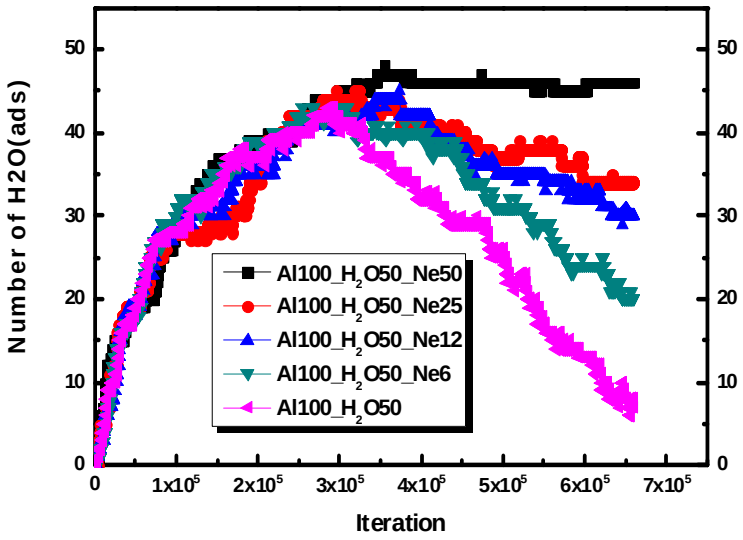

Figure **3-28**: Variation of the number of adsorbed water molecules on Al cluster for different Ne gas concentration cases

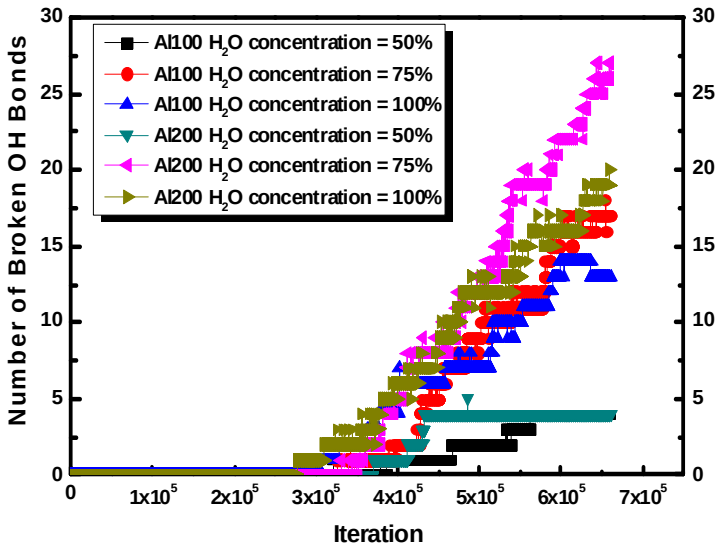

Figure **3-29**: Variation of the number of broken OH bonds for Al100 and Al200 cluster under different water concentrations

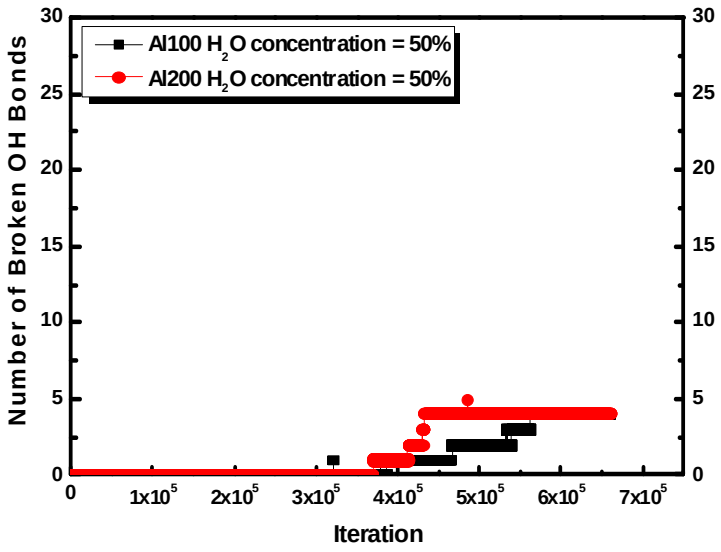

Figure **3-30**: Variation of the number of broken OH bonds for Al100 and Al200 clusters when water concentration is 50%.

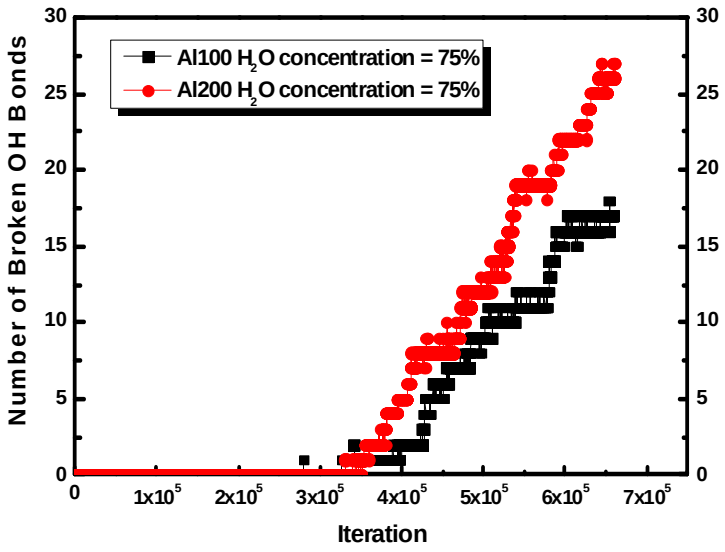

Figure **3-31**: Variation of the number of broken OH bonds for Al100 and Al200 clusters when water concentration is 75%.

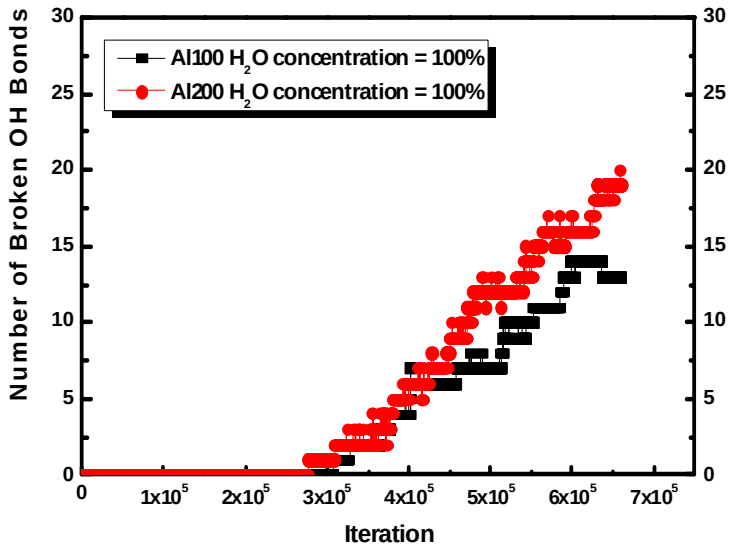

Figure **3-32**: Variation of the number of broken OH bonds for Al100 and Al200 clusters when water concentration is 100%.

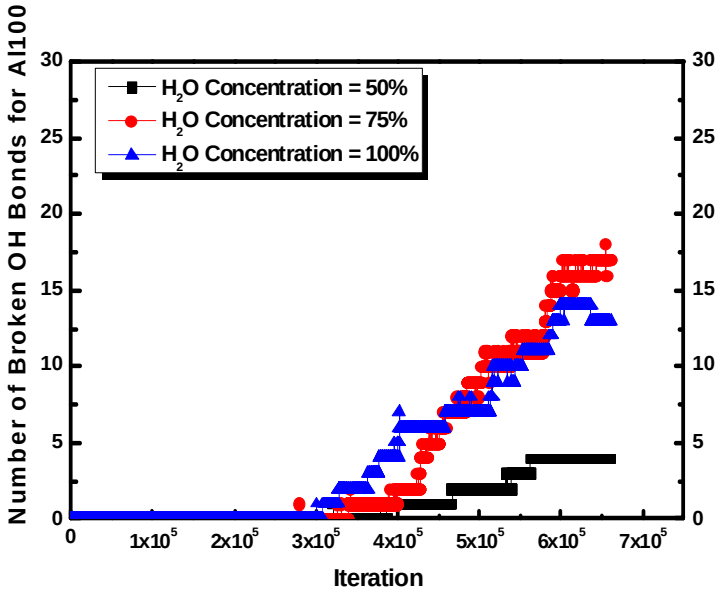

Figure **3-33**: Variation of the number of broken OH bonds for Al100 under different water concentrations

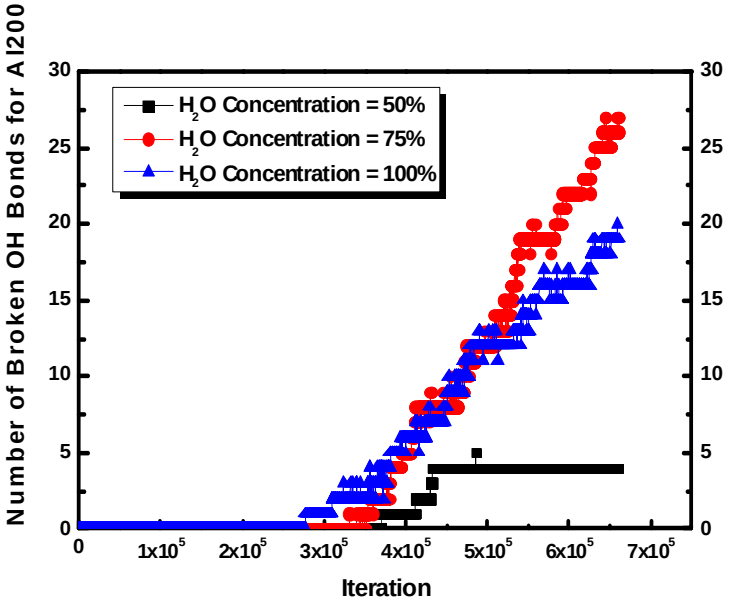

Figure **3-34**: Variation of the number of broken OH bonds for Al200 cluster under different water concentrations

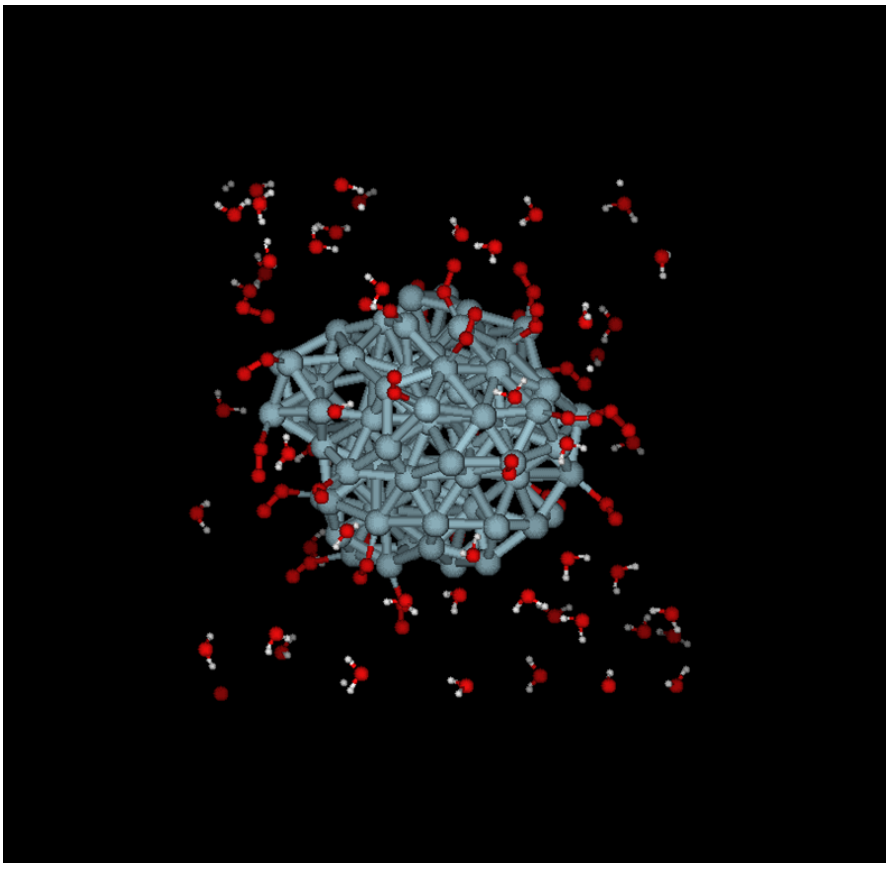

Figure **3-35**: Initial structure of aluminum cluster with aluminum oxide layer for case Al100_$O_2$25_H_2O50 (Gray: Al atoms, Red: oxygen atoms, White: hydrogen atoms)

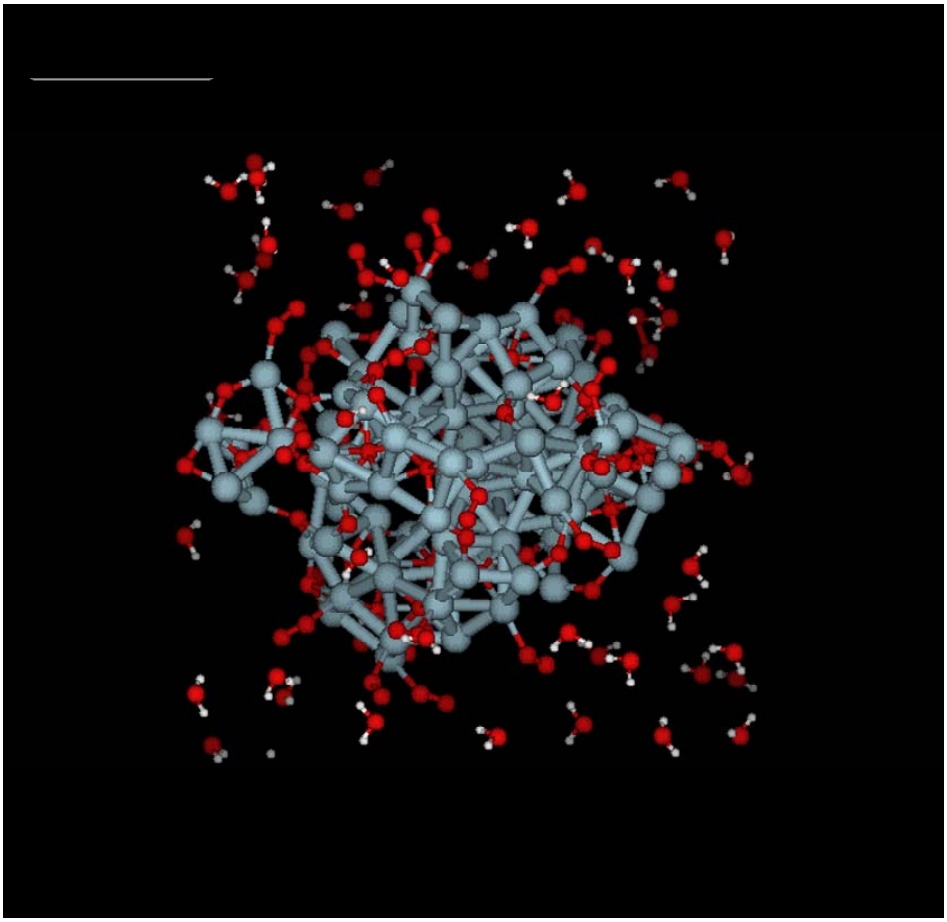

Figure **3-36**: Initial structure of aluminum cluster with aluminum oxide layer for case Al100_$O_2$50_H_2O50 (Gray: Al atoms, Red: oxygen atoms, White: hydrogen atoms)

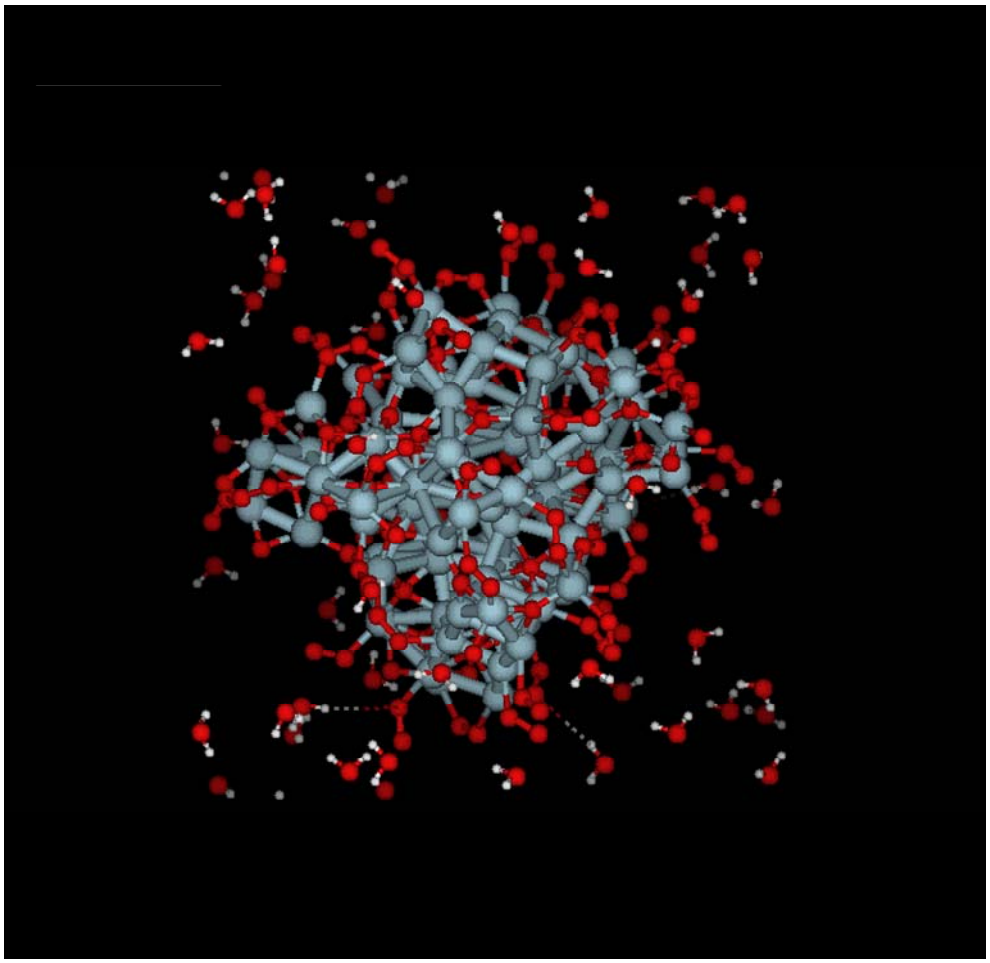

Figure **3-37**: Initial structure of aluminum cluster with aluminum oxide layer for case Al100_$O_2$79_H_2O50 (Gray: Al atoms, Red: oxygen atoms, White: hydrogen atoms)

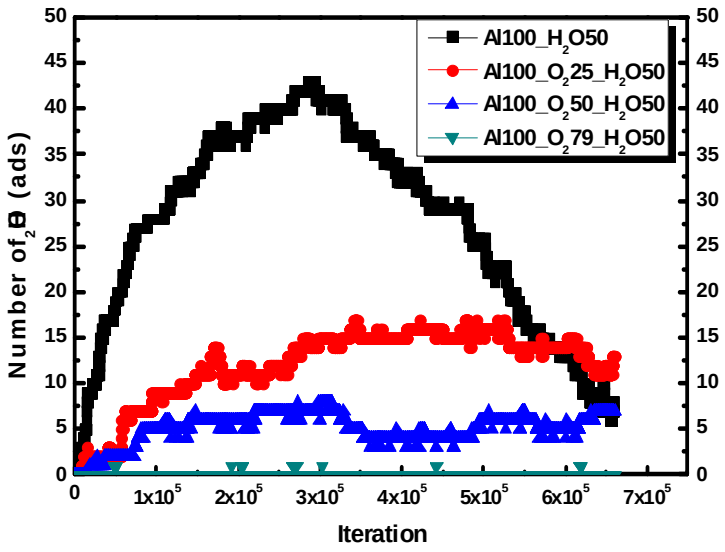

Figure **3-38**: Variation of the number of adsorbed water molecules on Al100 cluster under different aluminum oxide layer thicknesses

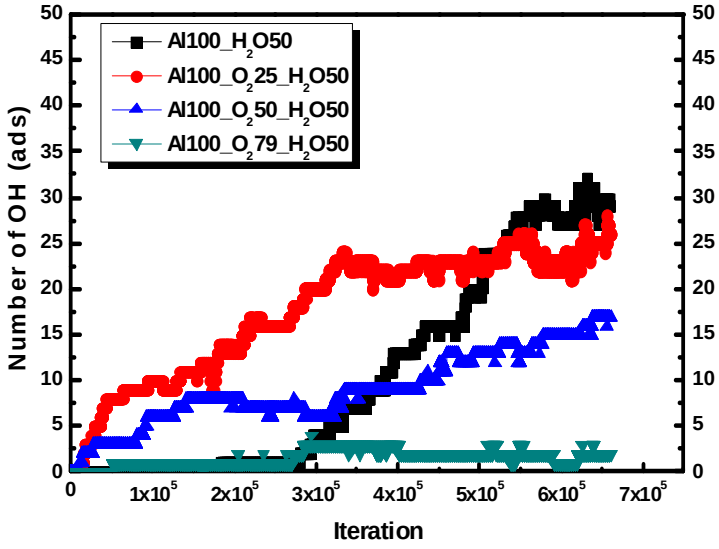

Figure **3-39**: Variation of the number of adsorbed hydroxyl on Al100 cluster under different aluminum oxide layer thicknesses

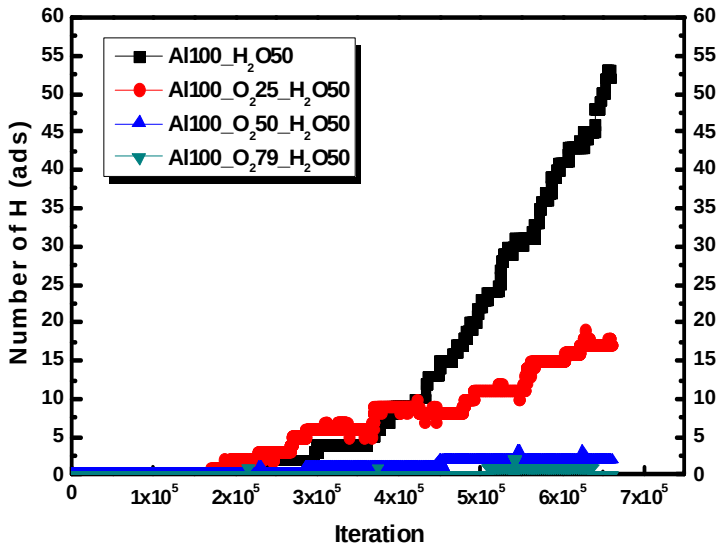

Figure **3-40**: Variation of the number of hydrogen atoms on Al100 cluster under different aluminum oxide layer thicknesses

Table 3-1: Simulation Cases for Temperature Influence Analysis

Simulation Case	Initial Temperature (K)		Temperature Increase/iteration		Heating Steps	Final Temperature (K)	
	Al	H_2O	Al	H_2O		Al	H_2O
Al100_H_2O50 (Case1)	0	0	0	0.005	330,000	0	1650
Al100_H_2O50_Heated (Case2)	300	300	0.005	0.005	290,000	1750	1750
Al100_H_2O50_Heated (Case3)	300	300	0.005	0.005	270,000	1650	1650

Table 3-2: Molecular Compositions at the End of Simulation for Temperature Influence Analysis

Simulation Case	H_2O (g)	H_2O (ads)	H_2O (dis)	H_2 (g)	H (ads)	OH (ads)	O (ads)	No. of Broken OH Bonds	Total Potential Drop （Kcal/mol）
Case 1 Al100_H_2O50	1	7	42	1	52	30	0	30	-2622.54
Case 2 Al100_H_2O50_Heated	5	29	16	0	31	1	15	15	-2916.76
Case 3 Al100_H_2O50_Heated	5	23	22	0	39	2	19	19	-3171.74

Table 3-3: Simulation Cases for Neon Gas Concentration Influences Analysis

Simulation Case	Initial Temperature (K)		Temperature Increase/iteration		Heating Steps	Final Temperature (K)	
	Al	H_2O and Ne	Al	H_2O and Ne		Al	H_2O and Ne
Case 1 Al100_H_2O50_Ne50	0	0	0	0.005	330,000	0	1650
Case 2 Al100_H_2O50_Ne25	0	0	0	0.005	330,000	0	1650
Case 3 Al100_H_2O50_Ne12	0	0	0	0.005	330,000	0	1650
Case 4 Al100_H_2O50_Ne6	0	0	0	0.005	330,000	0	1650
Case 5 Al100_H_2O50	0	0	0	0.005	330,000	0	1650

Table 3-4: Molecular Compositions at the End of Simulation for Ne Gas Concentration Influence Analysis

Simulation Case	H_2O (g)	H_2O (ads)	H_2O (dis)	H_2 (g)	H (ads)	OH (ads)	O (ads)	No. of Broken OH Bonds	Total Potential Drop （Kcal/mol）
Case 1 Al100_H_2O50_Ne50	0	46	4	0	4	4	0	4	-1344.03
Case 2 Al100_H_2O50_Ne25	1	34	15	3	10	14	1	16	-1805.94
Case 3 Al100_H_2O50_Ne12	0	30	20	2	18	17	0	17	-1620.66
Case 4 Al100_H_2O50_Ne6	2	20	28	0	32	24	4	32	-2348.03
Case 5 Al100_H_2O50	1	7	42	1	52	29	12	53	-2622.54

Table 3-5: Simulation Cases for Al Cluster Size Influences Analysis (Al100)

Simulation Case	Initial Temperature (K)		Temperature Increase/iteration		Heating Steps	Final Temperature (K)	
	Al	H_2O and Ne	Al	H_2O and Ne		Al	H_2O and Ne
Al100_H_2O50 _Ne50	0	0	0	0.005	330,000	0	1650
Al100_H_2O75 _Ne25	0	0	0	0.005	330,000	0	1650
Al100_H_2O100 _Ne0	0	0	0	0.005	330,000	0	1650

Table 3-6: Simulation Cases for Al Cluster Size Influences Analysis (Al200)

Simulation Case	Initial Temperature (K)		Temperature Increase/iteration		Heating Steps	Final Temperature (K)	
	Al	H_2O and Ne	Al	H_2O and Ne		Al	H_2O and Ne
Al200_H_2O80 _Ne80	0	0	0	0.005	330,000	0	1650
Al100_H_2O120 _Ne40	0	0	0	0.005	330,000	0	1650
Al100_H_2O160 _Ne0	0	0	0	0.005	330,000	0	1650

Table **3-7**: Simulation Cases for Aluminum Oxide Layer Influences Analysis

Simulation Case	Initial Temperature (K)		Temperature Increase/iteration		Heating Steps	Final Temperature (K)	
	Al and Al_xO_y	H_2O	Al and Al_xO_y	H_2O		Al and Al_xO_y	H_2O
Case 1 Al100_H_2O50	0	0	0	0.005	330,000	0	1650
Case 2 Al100_$O_2$25_H_2O50	0	0	0	0.005	330,000	0	1650
Case 3 Al100_$O_2$50_H_2O50	0	0	0	0.005	330,000	0	1650
Case 4 Al100_$O_2$79_H_2O50	0	0	0	0.005	330,000	0	1650

Table **3-8**: Molecular Compositions at the End of Simulation for Aluminum Oxide Layer Influences Analysis

Simulation Case	H_2O (g)	H_2O (ads)	H_2O (dis)	H_2 (g)	H (ads)	OH (ads)	O (ads)	Total Potential Drop （Kcal/mol）
Case 1 Al100_H_2O50	1	7	42	1	52	30	0	-2622.54
Case 2 Al100_$O_2$25_H_2O50	11	13	26	1	17	26	40	-7017.36
Case 3 Al100_$O_2$50_H_2O50	25	7	36	3	2	17	62	-3054.73
Case 4 Al100_$O_2$79_H_2O50	41	0	9	0	0	2	72	-952.98

Chapter 4

Conclusions and Future Work

4.1 Conclusions

In this work, the aluminum-water reaction was studied at nano-scale through molecular dynamic modeling integrated with ReaxFF, in which the reactive force field parameters were successfully optimized for aluminum and aluminum oxide. The following conclusions were obtained and summarized below.

The initial interactions between water molecules and the Al cluster is the adsorption of water molecules to the Al cluster and subsequently the dissociation of adsorbed water molecules. Water molecules in the gas phase assist the dissociation of adsorbed water molecules due to the interactions between them. At the same time, the adsorbed water molecules tend to connect with other water molecules in the gas phase forming water layers, which block the pathway for the reactants to arrive at the cluster surface and cover up available surface reaction sites. This phenomenon is termed as water molecule self poisoning. Due to reaction assistance as well as self poisoning effect of water molecules, the conversion rate of water molecules first increases and then decreases with the concentration of water molecules participating in the reaction.

Among the intermediate species generated during the reaction, the hydronium ion H_3O (cation) is considered to be important. It has three identical hydrogen atoms and is capable of reacting with water molecules which are both in the gas phase and adsorbed to the Al cluster. The hydronium ion assists the dissociation of water molecules, and it is an important intermediate in the aluminum-water reaction system.

Noble gas Neon was applied in aluminum-water reaction to control water concentration and water dissociation rate. Acting as inert specie, Ne atoms simply bounce around in the system and do not react with aluminum cluster, water molecules, or intermediated species. The direct collisions between Ne atoms and water molecules are not observed. The presence of Ne atoms, bouncing around in the system helps break the connection between the water molecules, which prevents the formation of water molecules layers and substantially helps attenuate water self poisoning effects. However, Ne atoms also adsorb some energy from aluminum-water reaction.

Therefore, as more Ne gas is applied, fewer adsorbed water molecules are dissociated. Regarding higher water molecule conversion rate, an optimum Ne gas concentration of 25% is observed, which is equivalent to an optimum water concentration of 75%.

The use of nano-sized metal particles in Al water reaction can offer significant advantages over larger size particles, due to the high specific surface area and overall small dimensions of nano-sized particles. Although the same average surface coverage of Al cluster by water molecules is maintained, more available surface reaction sites are provided by Al200, which represents for the Al cluster consisting of 200 Al molecules, than Al100 (Al cluster consists of 100 Al molecules). As a result, dissociation of adsorbed water molecules is assured by more available surface sites into which intermediate species move. The same optimum water concentration relative to higher water conversion rate is observed for both Al100 and Al200 clusters.

An aluminum oxide layer covering the cluster surface was also investigated. It causes the loss of available surface reaction sites. As a result, the adsorption of water molecules to Al cluster and the subsequent dissociation process are hindered. As the oxide layer becomes thicker, the spontaneous reaction of aluminum and water is prohibited or even completely stopped.

4.2 Future Work

Over the past few years, it is becoming more likely that the emphasis on cleaner fuel will lead to the use of hydrogen in a significant way. Therefore, hydrogen generation from inexpensive simple processes, of which aluminum-water reaction is promising one, are becoming increasingly important. Fundamental understanding about aluminum-water reaction is crucial for future applications of this reaction. Through the simulations in this work, the reaction mechanism of water molecules and the influences of noble gas on aluminum-water reaction are studied and understood. Still, much is left for future study.

The influences of aluminum cluster size on its reaction with water were observed through the simulation results of Al100 and Al200 clusters. More research can be conducted on other nano-sized Al clusters. Obviously, increasing Al cluster size would demand more computational time for both the annealing process and the following reaction simulation.

Besides cluster size, understanding how a specific shape or structure will affect the affinity of Al cluster toward water molecule may facilitate future efforts to design either stable or

reactive materials for specific technological applications. Research about the cluster shape or structure, or selectivity of specific reaction sites of aluminum cluster is also important for studying aluminum-water reaction.

Activation methods for aluminum-water reaction have always been and will continue to draw research interests concerning with the future applications of this reaction. Applying molecular dynamic modeling integrated with proper ReaxFF will allow us to study the following activation methods:

a) Modify aluminum cluster structure or cluster surface configuration,
b) Modify aluminum cluster through the addition of other materials, for example, a layer of other metal particles or certain compounds,
c) Study mechanical or chemical approaches to break or remove aluminum oxide layer on the cluster surface.

Appendix A

Reference

1. Shireen Meher Kotay, Debabrata Das, Biohydrogen as a renewable energy resource—Prospects and potentials, International Journal of Hydrogen Energy 33 (2008) 258-263
2. Palmer, D. (13 September 1997). "Hydrogen in the Universe". NASA. Retrieved 2008-02-05
3. Thorsteinn I. Sigfussion, Pathways to hydrogen as an energy carrier, Philosophical Transactions of the Royal Society A (2007) 365, 1025 – 1042
4. Nitsch, J. & Winter, C. J., Hydrogen as an energy carrier, technologies, systems and economy, Berlin, Germany: Springer, 1988
5. U.S. Census. 2006. <http://www.uscensus.gov>
6. Earth Policy. 2006. <http://earth-policy.org/Updates/Update45_data.htm>
7. Silberud R. Our future is hydrogen. Wellington, CO: New Science Publications; 2001
8. Meng Ni, Dennis Y.C. Leung, Michael K.H. Leung, K. Sumathy, An overview of hydrogen production from biomass, Fuel Processing Technology 87 (2006) 461 – 472
9. Dutton A. G. 2002 Hydrogen energy technology, Tyndall Working Paper TWP 17. Tyndall Centre for Climate Change, p. 30. Available from: http://www.tyndall.ac.uk/publications/working_ papers/wp17.pdf
10. Ewan, B. C. R. & Allen, R. W. K. 2005. A figure of merit of the routes to hydrogen, International Journal of Hydrogen Energy 30, 809 – 819
11. Meng Ni, Michael K.H. Leung, Dennis Y.C. Leung, K. Sumathy, A review and recent developments in photocatalytic water-splitting using TiO2 for hydrogen production, Renewable and Sustainable Energy Reviews 2007; 11: 401 – 425
12. Dragica Lj. Stojic, Milica P. Marceta, Sofija P., Hydrogen generation from water electrolysis—possibilities of energy saving, Journal of Power Sources 2003; 118: 315–319
13. H.Z. Wang, D.Y.C. Leung, M.K.H. Leung, M. Ni, A review on hydrogen production using aluminum and aluminum alloys, Renewable and Sustainable Energy Reviews 2009; 13: 845–853
14. Wegner K, Ly HC, Weiss R J, Pratsinis SE, Steinfeld A. In situ formation and hydrolysis of Zn nanoparticles for H2 production by the 2-step ZnO/Zn water-splitting thermochemical

cycle, International Journal of Hydrogen Energy 2006; 31: 55–61

15. Vishnevetsky I, Epstein M. Production of hydrogen from solar zinc in steam atmosphere, International Journal of Hydrogen Energy 2007; 32: 2791–802
16. Cho CY, Wang KH, Uan JY. Evaluation of a new hydrogen generating system: Ni-rich magnesium alloy catalyzed by platinum wire in sodium chloride solution, Materials Transactions 2005; 46 (12): 2704–8
17. Grosjean MH, Zidoune M, Roue L, Huot JY. Hydrogen production via hydrolysis reaction from ball-milled Mg-based materials, International Journal of Hydrogen Energy 2006; 31: 109–19
18. Grosjean MH, Roue L. Hydrolysis of Mg–salt and MgH2–salt mixtures prepared by ball milling for hydrogen production, Journal of Alloys and Compounds 2006; 416: 296–302
19. Uan JY, Cho CY, Liu KT. Generation of hydrogen from magnesium alloy scraps catalyzed by platinum-coated titanium net in NaCl aqueous solution, International Journal of Hydrogen Energy 2007; 32: 2337–43
20. Martınez SS, Benıtes WL, Gallegos AAA, Sebastian PJ. Recycling of aluminum to produce green energy, Solar Energy Materials and Solar Cells 2005; 88:237–43
21. Kravchenko OV, Semenenko KN, Bulychev BM, Kalmykov KB. Activation of aluminum metal and its reaction with water, Journal of Alloys and Compounds 2005; 397:58–62
22. Vargel C. Corrosion of aluminum. Oxford: Elsevier Ltd; 2004
23. U.S. Department of Energy, Reaction of Aluminum with Water to Produce Hydrogen, A study of Issues Related to the Use of Aluminum for On-Board Vehicular Hydrogen Storage, Version 1.0-2008
24. U.S. Patent 4, 308, 248; Material and method to dissociate water; December 29, 1981; Inventor: Eugene R. Anderson; Assignee: Horizon Manufacturing Corporation
25. U.S. Patent 6, 506, 360; Method for producing hydrogen; January 14, 2003; Inventors: Erling Reidar Andersen, Erling Jim Andersen; Assignee: None listed
26. U.S. Patent 6, 638, 493; Method for producing hydrogen; October 28, 2003; Inventors: Erling Reidar Andersen, Erling Jim Andersen; Assignee: None listed
27. U.S. Patent 6, 800, 258; Apparatus for producing hydrogen; October 5, 2004; Inventors: Erling Reidar Andersen, Erling Jim Andersen; Assignee: None listed
28. U.S. Patent 7, 144, 567; Renewable energy carrier system and method; December 5, 2006; Inventor: Erling Jim Andersen; Assignee: None listed
29. Brindley GF. Composition of matter for generating hydrogen. US Patent 909536, 1909.

30. Brindley GF, Bennie M. Composition of matter for manufacturing hydrogen gas. US Patent 934036, 1909.
31. Gill GC. Hydrogen generator. US Patent 2721789, 1955.
32. Checketts JH. Hydrogen generation pelletizaed fuel. US Patent 5728464, 1998.
33. Checkettes JH. Hydrogen generation system and pelletized fuel. US Patent 5817157, 1998.
34. Andersen ER, Andersen EJ. Method for producing hydrogen. US Patent 6506360, 2003.
35. Andersen ER, Andersen EJ. Apparatus for producing hydrogen. US Patent 2003/0118505 A1, 2003.
36. Andersen ER. Renewable energy carrier system and method. US Patent 2004/0115125 A1, 2004.
37. Hiraki T, Yamauchi S, Iida M, Uesugi H, Akiyama T. Process for recycling waste aluminum with generation of high-pressure hydrogen, Environmental Science & Technology 2007;41: 4454–7
38. Hiraki T, Takeuchi M, Hisa M, Akiyama T. Hydrogen production from waste aluminum at different temperatures with LCA, Materials Transactions 2005; 46(5): 1052–7
39. Belitskus D. Reaction of aluminum with sodium hydroxide solution as a source of hydrogen, Journal of the Electrochemical Society 1970; 117(8): 1097–9
40. Soler L, Macana´s J, Munoz M, Casado J. Hydrogen generation from aluminum in a non-consumable potassium hydroxide solution, Proceedings of International Hydrogen Energy Congress and Exhibition IHEC 2005, 13–15 July 2005, Istanbul, Turkey
41. Stockburger D, Stannard JH, Rao BML, Kobasz W, Tuck CD. On-line hydrogen generation from aluminum in an alkaline solution, Proceedings and Symposiums on Hydrogen Storage Materials, Batteries and Electrochemistry 1992; 92 (5): 431–44
42. Aleksandrov YA, Tsyganova EI, Pisarev AL. Reaction of aluminum with dilute aqueous NaOH solutions, Russian Journal of General Chemistry 2003;73(5):689–94
43. Soler L, Macana´s J, Mun˜oz M, Casado J. Aluminum and aluminum alloys as sources of hydrogen for fuel cell applications, Journal of Power Sources 2007;169(1):144–9
44. Z-Y Deng, J.M.F. Ferreira, Y. Tanaka, and J. Ye, Physicochemical Mechanism for the Continuous Reaction of γ-Al2O3-Modified Aluminum Powder with Water, Journal of the American Ceramic Society, 2007; 90, 1521–1526
45. International Patent Application PCT/CA2001/001115; Hydrogen generation from water split reaction; February 21, 2002; Inventors: Asoke Chaklader, Das Chandra; Assignee: The University of British Columbia

46. U.S. Patent 6,440,385; Hydrogen generation from water split reaction; August 27, 2002; Inventor: Asok C.D. Chaklader; Assignee: The University of British Columbia
47. U.S. Patent 6,582,676; Hydrogen generation from water split reaction; June 24, 2003; Inventor: Asoke Chandra Das Chaklader; Assignee: The University of British Columbia
48. A.G. Munoz and J.B. Bessone, Pitting of aluminum in non-aqueous chloride media, Corrosion Science, 1999; 41, 1447- 1463
49. E. McCafferty, Sequence of steps in the pitting of aluminum by chloride ions, Corrosion Science, 2003; 45, 1421-1438
50. International Patent Application PCT/CA2005/000546; Compositions and methods for generating hydrogen from water; October 20, 2005; Inventors: Tomasz Troczynski, Edith Czech; Assignee: The University of British Columbia
51. International Patent Application PCT/CA2006/001300; Microporous metals and methods for hydrogen generation from water split reaction; February 15, 2007; Inventors: Tomasz Troczynski, Edith Czech; Assignee: The University of British Columbia
52. Loup Verlet, Computer "experiments" on classical fluids. Ⅰ. Thermodynamical properties of Lennard-Jones molecules, Physical Review. 1967; 159, 98-103
53. Kimberly Chenoweth, Adri C. T. van Duin, and William A. Goddard, III, ReaxFF Reactive Force Field for Molecular Dynamics Simulations of Hydrocarbon Oxidation, Journal of Physical Chemistry A 2008; 112: 1040-1053
54. Van Duin, A., Dasgupta, S, Lorant, F., Goddard, W. A., III, ReaxFF: a reactive force field for hydrocarbons, Journal of Physical Chemistry A 2001, 105: 9396-9409
55. Strachan, A., van Duin, A., Chakraborty, D., Dasgupta, S., Goddard, W. A., III, Shock waves in high-energy materials: the initial chemical events in nitramine RDX, Physical Review. Letters, 2003; 91: 098301
56. Van Duin, A., Strachan, A., Stewman, S., Zhang, Q., Xu, X., Goddard, W. A., III, $ReaxFF_{SiO}$ reactive force field for silicon and silicon oxide systems, Journal of Physical Chemistry A, 2003; 107: 3803
57. Zhang, Q., Cagin, T., van Duin, A., Goddard, W. A., III, Qi, Y., Hector, L. G., Jr., Adhesion and nonwetting-wetting transition in the Al/alpha-Al_2O_3 interface, Physical Review B, 2004; 69: 045423
58. Patrick J. Roach, et al, Complementary active sites cause size-selective reactivity of aluminum cluster anions with water, Science, 2009; 323: 492

59. K. K. Kuo, Principles of Combustion, second edition, 2005

Appendix B

Cost Evaluation for Hydrogen Generation from Metal Water Reaction

In order to analyze whether it is cost competitive to use metal water reaction to produce hydrogen as the energy source compared to the conventional fossil fuels, the cost of hydrogen generation from metal water reaction is also calculated in the form per gallon of gas equivalent.

It is assumed that the combustion of methane is in 5% excess air at 2000K and 1atm, and the equivalence ratio Φ is 0.95. Then the coefficient for air in the combustion reaction is calculated as:

$$a = \frac{x + y/4}{\Phi} = \frac{1 + 4/4}{0.95} = 2.1 \tag{A-1}$$

The combustion reaction can be written as:

$$CH_4 + 2.1(O_2 + 3.76N_2) \rightarrow CO_2 + 2H_2O + 0.2O_2 + 7.896N_2 \tag{A-2}$$

Heat of reaction $\Delta H_{r,T}$ can be calculated according to [59], which is:

$$\Delta H_{r,T} = \Delta H_{r,T_0} + \sum_{i=1}^{N} \nu_i^{"} \int_{T_0}^{T} C_{P,i} dT - \sum_{i=1}^{N} \nu_i^{'} \int_{T_0}^{T} C_{P,i} dT \tag{A-3}$$

$$\Delta H_{r,T} = \Delta H_{r,T_0} + \sum_{\mathrm{Products}} \left(H_T - H_{T_0} \right) - \sum_{\mathrm{Reactants}} \left(H_T - H_{T_0} \right) \tag{A-4}$$

The first term on the right hand side of equation (A-4) $\Delta H_{r,T_0}$ can be calculated using:

$$\Delta H_{r,T_0} = \sum_{i=1}^{N} \nu_i^{"} \Delta h_{f,i}^{0} - \sum_{i=1}^{N} \nu_i^{'} \Delta h_{f,i}^{0} \tag{A-5}$$

$$\Delta H_{r,T_0} = 1 \times \Delta h_{f,CO_2}^{0} + 2 \times \Delta h_{f,H_2O}^{0} - 1 \times \Delta h_{f,CH_4}^{0} \tag{A-6}$$

$$\Delta H_{r,T_0} = -1 \times 94.054 - 2 \times 57.598 - 17.895$$

$$\Delta H_{r,T_0} = -227.545 Kcal$$

The second term on the right hand side of equation (A-4) is obtained as:

$$\sum_{\mathrm{Products}} \left(H_T - H_{T_0} \right) \tag{A-7}$$

$$\sum_{Products}\left(H_T - H_{T_0}\right)$$
$$= \left(H_T - H_{T_0}\right)_{CO_2} + 2\times\left(H_T - H_{T_0}\right)_{H_2O}$$
$$+ 0.2\times\left(H_T - H_{T_0}\right)_{O_2} + 7.896\times\left(H_T - H_{T_0}\right)_{N_2}$$
$$= 21.854 + 2\times 17.397 + 0.2\times 14.143 + 7.896\times 13.417$$
$$= 165.417 Kcal$$

Similarly, the third term on the right hand side of equation (A-4) is:

$$\sum_{Reactants}\left(H_T - H_{T_0}\right)$$
$$= \left(H_T - H_{T_0}\right)_{CH_4} + 2.1\times\left(H_T - H_{T_0}\right)_{O_2} + 7.896\times\left(H_T - H_{T_0}\right)_{N_2} \quad \text{(A-8)}$$
$$= 29.539 + 2.1\times 14.143 + 7.896\times 13.417$$
$$= 165.180 Kcal$$

Hence, the heat of reaction of methane combustion under specified condition is:

$$\Delta H_{r,T}^{CH_4} = \Delta H_{r,T_0} + \sum_{Products}\left(H_T - H_{T_0}\right) - \sum_{Reactants}\left(H_T - H_{T_0}\right) \quad \text{(A-9)}$$
$$\Delta H_{r,T}^{CH_4} = -227.545 + 165.417 - 165.180$$
$$\Delta H_{r,T}^{CH_4} = -227.308 Kcal$$

Similarly, the heat of reaction of hydrogen combustion at T=2000K and P=1atm can be calculated. The reaction is:

$$H_2 + \frac{1}{2}O_2 = H_2O \quad \text{(A-10)}$$

Heat of reaction $\Delta H_{r,T}$ can be calculated from:

$$\Delta H_{r,T} = \Delta H_{r,T_0} + \sum_{i=1}^{N} \nu_i^{"} \int_{T_0}^{T} C_{P,i} dT - \sum_{i=1}^{N} \nu_i^{'} \int_{T_0}^{T} C_{P,i} dT \quad \text{(A-11)}$$

$$\Delta H_{r,T} = \Delta H_{r,T_0} + \sum_{Products}\left(H_T - H_{T_0}\right) - \sum_{Reactants}\left(H_T - H_{T_0}\right) \quad \text{(A-12)}$$

The first term on the right hand side of equation (A-12) $\Delta H_{r,T_0}$ is:

$$\Delta H_{r,T_0} = \sum_{i=1}^{N} \nu_i^{"} \Delta h_{f,i}^0 - \sum_{i=1}^{N} \nu_i^{'} \Delta h_{f,i}^0$$
$$\Delta H_{r,T_0} = \Delta h_{f,H_2O}^0 \quad \text{(A-13)}$$
$$\Delta H_{r,T_0} = -57.598 Kcal$$

The second and third terms on the right hand side of equation (A-12) are:

$$\sum_{\text{Products}} \left(H_T - H_{T_0}\right) = \left(H_T - H_{T_0}\right)_{H_2O} = 17.397 Kcal \tag{A-14}$$

$$\sum_{\text{Reactans}} \left(H_T - H_{T_0}\right) = \left(H_T - H_{T_0}\right)_{H_2} + 0.5 \times \left(H_T - H_{T_0}\right)_{O_2} \tag{A-15}$$
$$= 12.656 + 0.5 \times 14.143 = 19.7275 Kcal$$

Hence, the heat of reaction of hydrogen combustion under specified condition is:

$$\Delta H_{r,T}^{H_2} = \Delta H_{r,T_0} + \sum_{\text{Products}} \left(H_T - H_{T_0}\right) - \sum_{\text{Reactants}} \left(H_T - H_{T_0}\right)$$
$$\Delta H_{r,T}^{H_2} = -57.798 + 17.397 - 19.7275 \tag{A-16}$$
$$\Delta H_{r,T}^{H_2} = -60.1285 Kcal$$

In order to provide the same amount of heat of reaction from hydrogen combustion as that of per mole of methane combustion, the mole of hydrogen needed is:

$$n_{H_2} = \frac{227.308}{60.129} = 3.780 mol \tag{A-17}$$

From aluminum water combustion reaction:

$$2Al + 6H_2O = 2Al\left(OH\right)_3 + 3H_2 \tag{A-18}$$

the amount of aluminum needed to produce 3.780 mol H_2 is found out to be

$$n_{Al} = \frac{2 \times 3.780}{3} = 2.52 mol \tag{A-19}$$

Assume in per gallon of gas, the mole fraction of methane is approximately 33%, the mole of methane in per gallon of gas is obtained ads

$$n_{CH_4} = \frac{\rho V}{M_{CH_4}} = \frac{162 \times 10^3 g/m^3 \times 3.7854 \times 10^{-3} m^3}{0.33 \times 16 g/mol} = 116.143 mol \tag{A-20}$$

Therefore, the amount of aluminum needed relative to per gallon of gas equivalent is:

$$m_{Al} = 2.52 \times 116.143 \times 27 = 7902.367 g \tag{A-21}$$

According to the latest price of aluminum, which is 1.441USD/kg, per gallon of gas equivalent is calculated when using aluminum-water reaction to produce hydrogen:

$$7902.367 \times 10^{-3} \times \$1.441 = \$11.387 \tag{A-22}$$

Therefore, per gallon of gas equivalent is $\$11.387$

The variation of per gallon of gas equivalent with aluminum price is described in Figure **A-1**, according to the historic price of aluminum for the latest 5 years from London Metal Exchange. Besides, Table **A-1** summarizes hydrogen generation from different metal water reactions.

Applying the same method as for aluminum-water reaction, the calculated per gallon of gas equivalent for each of the metal is listed in Table **A-1**. As shown in Figure **A-2**, aluminum is the second cheapest metal analyzed for hydrogen generation from metal water reaction.

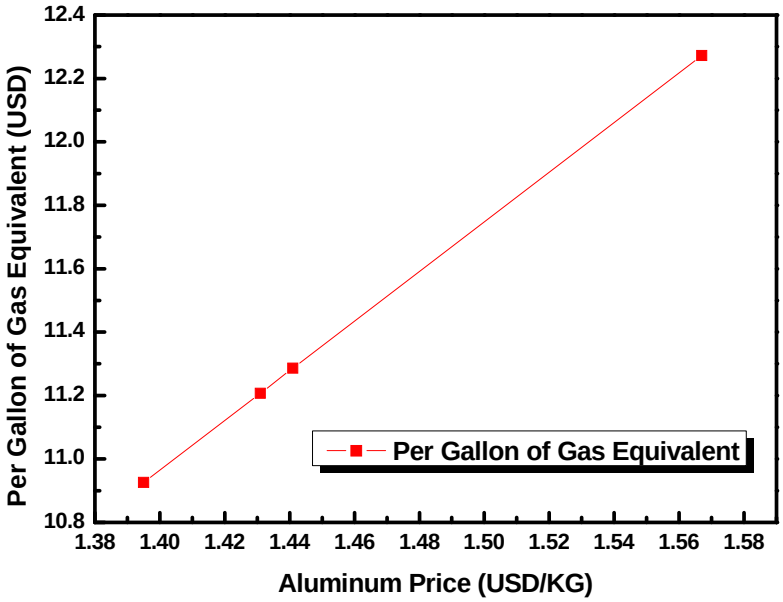

Figure **A-1**: Per gallon of gas equivalent of hydrogen generation from aluminum-water reaction versus aluminum price

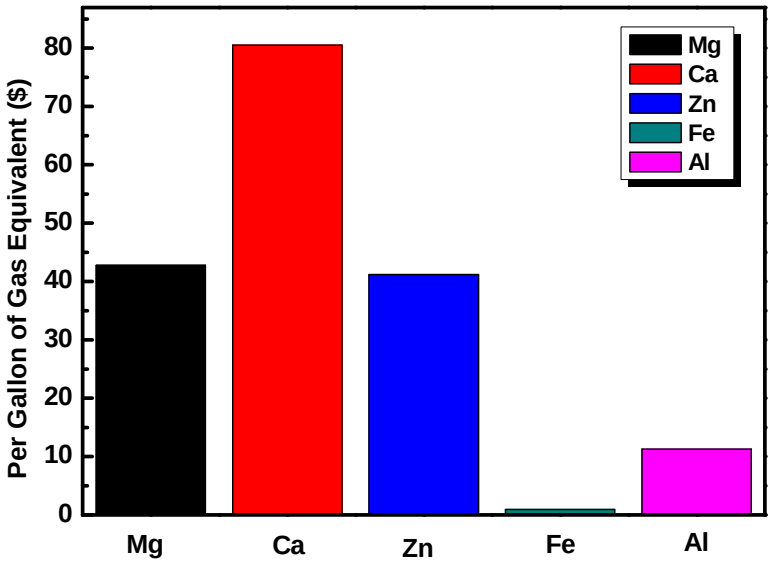

Figure **A-2**: Cost of per gallon of gas equivalent for hydrogen generation from different metal water reactions

Table **A-1**: Summary of Metal Water Reactions

Metal	Reaction	Price ($/KG)	Per Gallon of Gas Equivalent ($/KG)
Mg	$Mg + H_2O \rightarrow MgO + H_2$	4.1	42.767
Ca	$Ca+2H_2O \rightarrow Ca(OH)_2 + H_2$	4.63	80.493
Zn	$Zn+H_2O \rightarrow ZnO+H_2$	1.46	41.161
Fe	$3Fe + 4H_2O \rightarrow Fe_3O_4 + 4H_2$	0.05	0.913